On the value of combined heat and power (CHP) systems and heat pumps in centralised and distributed heating systems: Lessons from multi-fidelity modelling approaches

Andreas V. Olympios[1], Antonio M. Pantaleo[1,2], Paul Sapin[1], Christos N. Markides[1,*]

[1] *Clean Energy Processes (CEP) Laboratory and Centre for Process Systems Engineering (CPSE), Department of Chemical Engineering, Imperial College London, London SW7 2AZ, UK*

[2] *Department of Agro-environmental Sciences, University of Bari, Via Orabona 3, 70125 Bari, Italy*

* Corresponding author: c.markides@imperial.ac.uk

A short version of this paper was presented at the 11th International Conference on Applied Energy (ICAE2019) held on 12-15 August 2019 in Västerås, Sweden [1]. This paper is a substantial extension of the short version of the conference paper.

N.B.: This is the ACCEPTED MANUSCRIPT version of this article. The final, published version of the article can be found at: https://doi.org/10.1016/j.apenergy.2020.115261.

ABSTRACT

This paper presents a multi-scale framework for the design and comparison of centralised and distributed heat generation solutions. An extensive analysis of commercially available products on the UK market is conducted to gather information on the performance and cost of a range of gas-fired combined heat and power (CHP) systems, air-source heat pumps (ASHPs) and ground-source heat pumps (GSHPs). Data-driven models with associated uncertainty bounds are derived from the collected data, which capture cost and performance variations with scale (*i.e.*, size and rating) and operating conditions. In addition, a comprehensive thermoeconomic (thermodynamic and component-costing) heat pump model, validated against manufacturer data, is developed to capture design-related performance and cost variations, thus reducing technology-related model uncertainties. The novelty of this paper lies in the use of multi-fidelity approaches for the comparison of the economic and environmental potential of important heat-generation solutions: (i) centralised gas-fired CHP systems associated with district heating network; (ii) gas-fired CHP systems or GSHPs providing heat to differentiated energy communities; and (iii) small-scale micro-CHP systems, ASHPs or GSHPs, installed at the household level. The pathways are evaluated for the case of the Isle of Dogs district in London, UK. A centralised CHP system appears as the most profitable option, achieving annual savings of £13M compared to the use of decentralised boilers and a levelised cost of heat equal to 31 £/MWh$_{th}$. However, if the carbon intensity of the electrical grid continues to reduce at current rates, CHP systems will only provide minimal carbon savings compared to boilers (<6%), with heat pumps achieving significant heat decarbonisation (55-62%). Differentiating between high- and low-specification and cost heat pump designs shows that the former, although 25% more expensive, have significantly lower annualised costs (£4.9M *vs.* £7.7M) and 12% higher CO_2-equivalent savings. The uncertainty propagation reveals that data-driven and detailed thermoeconomic models can reduce the uncertainty in the total annualised energy cost and emissions by more than 75% compared to simplified black-box approaches, while the economic comparison of centralised CHP systems and domestic heat pumps for various electricity and gas price scenarios provides guidance to support energy policy.

Keywords: combined heat and power, cogeneration, distributed energy, district heating, heat pumps, heating, urban energy systems.

Nomenclature

Abbreviations

ASHP	air-source heat pump
CAPEX	capital expenses
CEPCI	chemical engineering plant cost index
CCC	Committee on Climate Change
CHP	combined heat and power
COP	coefficient of performance
DECC	Department of Energy & Climate Change
DH	district heating
GLUD	generalised land use database
GSHP	ground-source heat pump
GWP	global warming potential
HEX	heat exchanger
ICE	internal combustion engine
KPI	key performance indicator
LCOH	levelised cost of heat
LMTD	log-mean temperature difference
MSOA	middle-layer super output area
PBT	payback period
PPTD	pinch-point temperature difference

Greek symbols

α	heat transfer coefficient ($Wm^{-2}K^{-1}$)
Δ	difference (-)
ε	relative uncertainty or variability (-)
η	efficiency (-)
λ	thermal conductivity ($Wm^{-1}K^{-1}$)
ρ	density (kgm^{-3})

Symbols

A	area (m^2)
C	cost (£)
c_p	specific heat capacity ($Jkg^{-1}K^{-1}$)
D	diameter (m)
$\mathfrak{D}$	demand (W)
d	degree (K)
E	energy (J, Wh)
$\mathcal{E}$	carbon emissions ($kgCO_{2(eq)}$)
h	specific enthalpy ($Jkg^{-1}K^{-1}$)
k_CF	carbon factor ($kgCO_{2(eq)}Wh^{-1}$)
k_OM	operation & maintenance factor (%)
l	length (m)
$\dot{m}$	mass flow rate (kgs^{-1})
N	number of units (-)
Nu	Nusselt number (-)
P	price (£/Wh)
Pr	Prandtl number (-)
PL	part load (-)
$\dot{Q}$	heat flow (W)
R	revenue (£)
Re	Reynolds number (-)
r_d	discount rate (%)
T	temperature (K)
t	time (h)
U	overall heat transfer coefficient ($W/m^{-2}K^{-1}$)
u	absolute uncertainty or variability (-)
V	volume (m^3)
$\dot{V}$	volume flow rate (m^3s^{-1})
v	velocity (ms^{-1})
$\dot{W}$	power (W)
x	wall thickness (m)

Subscripts

ann	annual
boil	boiler
cap	capital
cb	convective boiling
comp	compressor
cond	condenser
cyl	cylinder
des	design point
EE	exported electricity
el	electricity
evap	evaporator
flow	flow in supply pipe
gas	natural gas
h	heat
i	increment
in	inlet/input
inner	side of working fluid
is	isentropic
j	technology
loss	loss to surroundings
max	maximum
min	minimum
nb	nucleate boiling
op	operational
out	outlet/output
outer	side of source/sink stream
PE	purchased electricity
p	peak
pipe	district heating pipe
pr	production
r	ratio
return	flow in return pipe
sav	savings
sc	subcooling
sh	superheating
sink	heat sink
src	heat source
t	hour
th	thermal
tot	total
w	water
wf	working fluid

1. Introduction

The UK has now passed laws aiming for net-zero greenhouse gas emissions by 2050 [2]. Unlike the recent advancements in renewable electricity generation with photovoltaics and wind generation experiencing increasing growth [3], emissions from space heating and hot water in residential and commercial sectors still account for as high as 83% of the total country's heating emissions [4]. Heat accounts for 44% of the country's energy consumption [5], demonstrating the urgency for redefining how heat is generated and delivered to consumers.

Meeting the world's increasing demand for heat and the associated wide-ranging and diverse challenges requires exploiting current and future energy resources in the most efficient, cost-effective and sustainable way possible. While heat and electricity networks had been traditionally relying on fossil fuels, burning coal, oil and gas, the energy mix is changing [6] and is highly influenced by climate change [7]. Identifying optimal decarbonisation pathways requires simulations that can capture trade-offs across multiple scales: from those between different ways of transporting energy to the those between possible technology options, components and operation strategies. Capturing the complex interactions between different technology choices and design options is necessary so that all stakeholders (system operators, component manufacturers, investors, end users) appreciate the optimal characteristics of the future energy infrastructure.

In energy-system modelling, the main aim is to analyse and compare different decarbonisation pathways that an area or country should follow to achieve their economic and environmental objectives. The study of possible low-carbon heat provision pathways is receiving increasing attention recently. Combusting gas in boilers is exergetically wasteful and the UK government has identified a range of low-carbon alternatives, including combined heat and power (CHP) technologies, heat pumps, solar heating, biomass boilers and hydrogen boilers [8]. These can be either installed centrally at large scales and be accompanied by district heating (DH) networks or in micro-units at the household level. To evaluate the different alternatives and analyse carbon budgets, the Department of Energy & Climate Change (DECC) and the Committee on Climate Change (CCC) make use of cost-optimising models like the UK MARKAL model [9,10] or the Integrated Whole-Energy System (IWES) model [11], which are technology-rich, linear-programming models portraying the entire energy system. Such models support system-wide policies and provide recommendations on how to invest in low-carbon heating technologies. The IWES model has been used to provide, along with the CCC, an assessment of the possible pathways to decarbonise heat: electric, hydrogen or a combination of both [11]. In the sensitivity analysis of that report, it was shown that slight changes in cost and performance assumptions of technologies and networks can result to different suggested pathways, concluding that no pathway can be excluded and that "the focus of any action should be to address uncertainties".

The combination of multiscale, multi-component and multi-process technologies in modelling efforts is complex, with challenges regarding issues of space, time, technology interactions and human behaviour being growing [12]. Many energy-system models focus on the effects of temporal and spatial resolution [13,14], while others capture aspects like human-decision making [15]. The model of Samsatli *et al.* [13, 14] is set around the availability of primary resources and simultaneously considers all possible energy vectors (*e.g.*, syngas, hydrogen, electricity), capturing short-term and long-term operation planning, while the MUSE [15] is an agent-driven model not aiming to capture the system dynamics, but to include another interesting aspect: each agent (individual) bases their investment decision on their own goals and preferred strategy. Furthermore, the Electricity Systems Optimisation (ESO) model [16], which was expanded to include endogenous technology cost reductions [17], demonstrates how the availability of low-carbon technologies can have an impact on the capacity mix of technologies of the near future.

Different energy-system models have their own strengths and they all convey important messages. However, all such models share a similar limitation: the cost and performance of competing technologies, especially with respect to heating, are represented by single values [11,13,14], or, in the best case, with the use of low-fidelity black-box models that rely on simple input-output mappings [15–17]. Such simplified technology-agnostic models cannot capture the dependence of the cost and performance of technologies on the size, component design and varying operating conditions (off-design or part-load). Therefore, the use of reduced-order models is associated with large uncertainties (*i.e.*, performance and cost variability), making it difficult to identify low-cost pathways reliably, and to provide manufacturers with insight into how to design technologies (*e.g.*, select materials and components) that are optimal in meeting economic and environmental objectives.

Heat is a particularly difficult energy vector to decarbonise. Internal combustion engine (ICE) CHP technologies and heat pumps have a large role to play in the venture for decarbonisation of heat [18–20]. The electrical and thermal efficiencies of ICE-CHP systems change significantly with scale [19] and part-load operation [21], while the specific cost drops drastically with scale. At the same time, heat pumps can involve different heat sources (*e.g.*, air and ground), while the choice of working fluid and the design of components (compressor, heat exchangers) largely affect cost and performance [20], which explains the large variety of designs and prices.

While the majority of electricity generation is based on centralised power plants, the employment of central heat-generation units and heat networks is very limited in the UK. In particular, CHP engines contribute to only about 15% of the heat supplied by DH networks [22]. The latter show significant potential in high energy-density areas [23]. Detailed pipe-network design and costing has been explored in the work of Pirouti *et al.* [24], while the work of Delangle *et al.* [25] presents a comparison of centralised CHP engines, water-source heat pumps, gas boilers and biomass boilers. Although the existing literature has explored various DH network design methodologies, low effort is being devoted to capturing the multi-process characteristics of the candidate technologies.

In light of the fact that small changes in technology-related assumptions lead to the proposal of very different decarbonisation pathways by whole-energy system models, the novelty of this paper lies in the use of multi-fidelity approaches for the comparison of the economic and environmental potential of possible heat-generation solutions. Three main contributions are made relative to previous efforts in the literature. Firstly, the work presents surrogate technoeconomic models that have been developed to capture the main variations (spread) in the performance and cost of existing ICE-CHP engines, air-source heat pumps (ASHPs) and ground-source heat pumps (GSHPs) at different scales/sizes and operating conditions. This is performed through an extensive analysis of commercially available products on the UK market, and involves collecting data for the cost and performance of CHP systems and heat pumps of various ratings from different UK manufacturers. Fitting techniques are used to determine relationships arising from the collected data, infer values for which data is not available and quantify the related uncertainty (*i.e.*, variability) in technology characteristics between the data and fitted relationships. These data-driven models provide useful information to energy-system modellers in their efforts to reduce simulation uncertainties and to suggest reliable system-wide strategies. The range in different heat-pump designs and prices found on the market is substantial, and this gives rise to a significant spread in the data, especially with respect to ASHP costs. Therefore, a thermoeconomic (thermodynamic and component-costing) vapour-compression ASHP model is developed to capture the major design-related performance and cost variations, thus reducing ASHP model uncertainties.

The second contribution of this work lies in the utilisation of the developed data-driven models to assess the economic and environmental performance of three heat decarbonisation pathways: (i) centralised large-scale generation accompanied by DH networks; (ii) medium-scale generation for differentiated energy communities; and (iii) decentralised, domestic-scale generation. This work includes spatially lumped modelling of the DH network. The trade-offs between centralised and distributed options are

examined using heating demand profiles, electricity price profiles and building data for a highly populated UK district, the Isle of Dogs in East London, and the use of technoeconomic models allows to choose optimal technology sizes and, in the case of ASHP, compare different possible designs.

Thirdly, an uncertainty propagation analysis is applied for the first time within a technology comparison analysis to demonstrate the significance of accounting for technology-related performance and cost variations. This is done by comparing the uncertainty in the resulting cost and emission predictions when using black-box, data-driven and detailed thermoeconomic (thermodynamic and component-cost) models, the latter in the case of ASHPs which are shown to exhibit the largest spread in performance and cost characteristics from the analysis of commercial products, in all cases arising from the variability and resulting deviations between actual data and model predictions.

Section 2 describes the main heat decarbonisation pathways and presents the developed data-driven and thermodynamic models, quantifying the associated uncertainty. A comparison of the pathways and the effect of uncertainty propagation are presented in Section 3, which also discusses the effect of gas and electricity prices in the pathway choice. Section 4 provides concluding remarks.

2. Methodology

The decarbonisation pathways considered in this paper are distinguished into three main categories, as shown in Fig. 1: (i) centralised generation through ICE-CHP systems and associated DH network; (ii) medium-scale generation through ICE-CHP systems or GSHPs for differentiated energy communities; and (iii) small-scale generation integrated in each home, through micro-CHP engines, small-scale ASHPs or GSHPs. In the first pathway, centralised large-scale CHP systems convert natural gas to heat and electricity, and DH networks transport heat to individual households. The second pathway involves local energy communities (groups of people living together, which can be as low as 20-30 inhabitants [26]) that produce heat locally and are able to function in islanded mode. DH networks are still required in the second pathway; however, the pipe sizing/length and costs/heat losses are different. In the third pathway, no DH network is required.

Although a complete analysis of heat decarbonisation options should also include other heat provision options, including other heat-pump types (*e.g.*, water-source, gas-driven, solar-assisted), as well as hydrogen boilers, fuel-cell cogeneration, solar thermal and hybrid photovoltaic-thermal collectors and biomethane, the intention here is not to provide a complete answer to the heat decarbonisation problem, but to consider the influence of model fidelity and to demonstrate how technoeconomic models of varying detail (data-driven, thermoeconomic) can be used to capture realistic technology characteristics, the uncertainties associated with different fidelity models, and how these uncertainties can propagate through wider energy-system models. Therefore, the framework developed and presented here does not describe a whole-energy system or provide an optimised strategic decarbonisation plan. However, it allows for an informed comparison of the (currently) most common heating technologies and options, and provides useful insights to energy-system modellers for quantifying and, where necessary, reducing simulation uncertainties in order to draw more reliable conclusions. Furthermore, certain technologies (*e.g.*, water-source or solar-assisted heat pumps) involve geographical constraints, which makes them more strongly subject to local conditions and less transferable to other regions and scenarios. This work focuses on the most common technologies that can be readily transferred across different regions.

The rest of this section describes how the economic and environmental performance of each option are evaluated and presents how technoeconomic models (data-driven and thermoeconomic) can capture realistic technology characteristics.

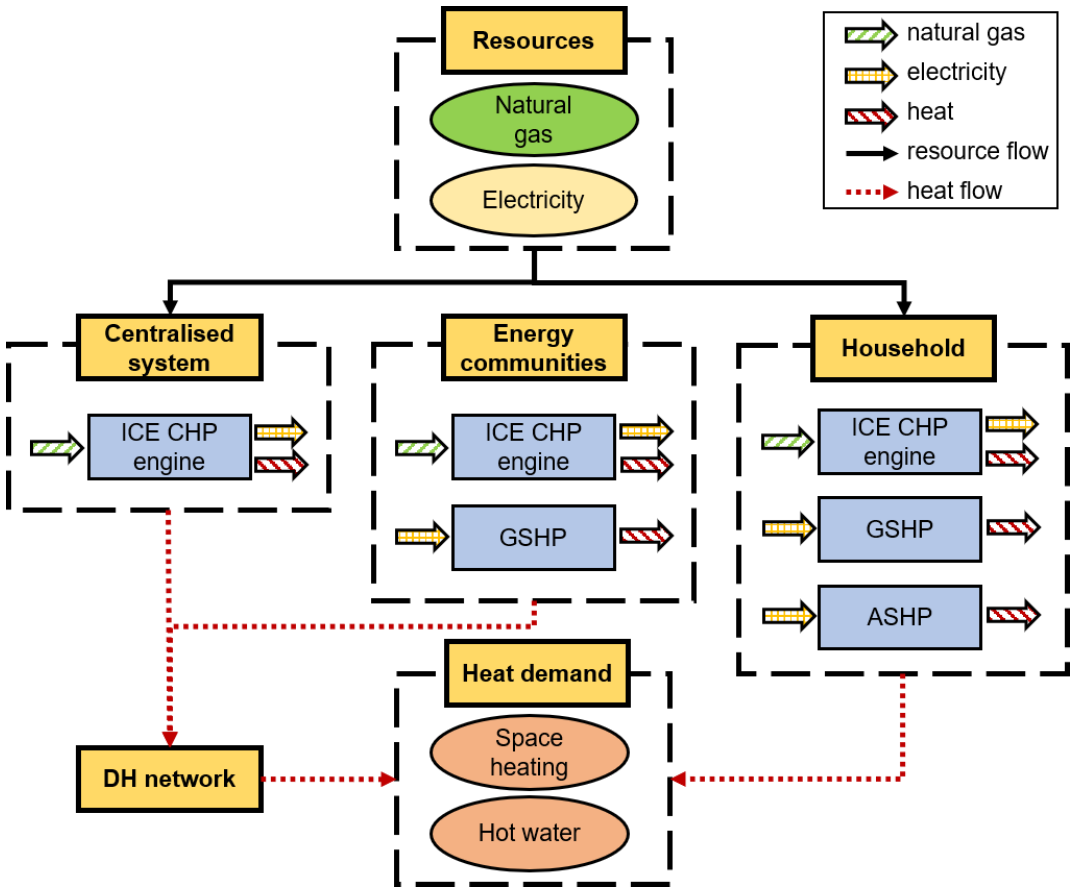


Figure 1. Schematic representation of pathways under investigation for the provision of heat. Centralised systems or systems installed at energy-community level require DH networks. CHP systems use natural gas to provide heat and electricity, while heat pumps use electricity to provide heat.

2.1. Description of pathways

In this work, each of the pathways is considered independently and the different centralised and distributed options are compared with respect to a set of key performance indicators (KPIs). Using data from the analysis of commercially available products on the UK market, a non-linear optimisation problem is developed to obtain the optimal size of the technology considered in each pathway. All optimisation problems are solved using MATLAB's interior point algorithm *fmincon* [27]. The model uses an hourly discretisation and an observed horizon of one year. It is assumed that the current production units are decentralised boilers. Natural gas is assumed to be imported at a specified fixed cost, while electricity can be exchanged with the grid using hourly importing and exporting prices. The carbon footprint of natural gas and hourly data for the carbon footprint of electricity are used to calculate carbon emission savings. The heat demand must always be met and the heat output of generation systems is never allowed to exceed demand, such that heat is never wasted. This is expressed using the heat balance equation:

$$\dot{Q}_{\mathfrak{D}} + \dot{Q}_{\mathrm{DH,loss}} = \sum_{j} \dot{Q}_{\mathrm{pr},j}\,, \tag{1}$$

where $\dot{Q}_{\mathfrak{D}}$ is the heat demand; $\dot{Q}_{\mathrm{DH,loss}}$ the constant DH network heat loss rate; and $\dot{Q}_{\mathrm{pr},j}$ the rate of heat production of each technology j.

2.1.1. Backup technologies and storage

In all pathways, backup technologies are included in the analysis to provide additional heat when required. These are sized according to:

$$\dot{Q}_{\mathfrak{D},\mathrm{peak}} + \dot{Q}_{\mathrm{DH,loss}} = \sum_{j} N_j \dot{Q}_{\mathrm{pr,max},j} \,, \tag{2}$$

where $\dot{Q}_{\mathfrak{D},\mathrm{peak}}$ is the peak thermal demand; $\dot{Q}_{\mathrm{pr,max},j}$ and N_j are the nominal thermal capacity and the number of units of each technology j, respectively.

Gas boilers are the backup technology for CHP systems. Whenever demand exceeds the maximum capacity of the CHP system, or whenever it falls below the minimum part-load level $\dot{Q}_{\mathrm{pr,min},j}$, the system is switched off and demand is met by the backup boilers. For each hour t:

$$\dot{Q}_{\mathrm{pr},j,t} < \dot{Q}_{\mathrm{pr,min},j} \,. \tag{3}$$

It is noted that there are wider costs, beyond and in addition to those associated with the installation of the heat-generating technology, which arise from the installation of alternative heating systems as replacements to existing systems [28], primarily due to thermal storage. Although detailed sizing, design and optimised operation (charging and discharging) of thermal stores is out of the scope of this present study, an additional cost is included to account for a hot-water store that is sized so that heating system can cover the peak demand for heat over a period of 1 hour.

In more detail, in the case of transitioning from the current heating scenario to a centralised heating system, large-scale hot water cylinders and backup boilers would be needed, whose installation would involve added costs, along with the cost of installing the district heating network infrastructure. These costs would be incurred independent of the centralised heat-generating technology.

Similarly, retrofitting a domestic central-heating system with a gas-fired boiler by installing a domestic heat pump would require the end-user to install a heat-pump compatible hot-water cylinder. Conventional hot water cylinders experience significant problems when integrated with heat pumps, due to the fact that heat pumps operate at lower temperatures than boilers and thus require larger heat exchanger coils [29, 30]. Therefore, heat decarbonisation pathways featuring heat pumps should incorporate the requirement for specific compatible hot water cylinders, which have larger heat exchanger coils than a conventional cylinder manufactured and installed in domestic central-heating systems. Most commercial hot water cylinders which are specifically designed to be integrated with heat pumps also include a small electric immersion heater, which can act as a backup technology, switching on whenever the heat pump is unable to provide all the heating demand.

On the other hand, the installation of domestic CHP systems would not incur additional costs for storage, since we consider that these systems can still use the existing hot-water stores, which are compatible with micro-CHP systems. It is therefore assumed here that in the case that these households are equipped with micro-CHP systems, the existing central-heating systems can be used for backup and storage purposes, therefore no additional technologies should be acquired, and no additional costs arise. These costs are detailed in Section 2.1.3.

2.1.2. District heating

Centralised technology options benefit from economies of scale and enhanced performance. However, associated DH networks involve significant costs. Calculating the cost and thermal loss of the network requires knowledge of the network length, as well as an estimate of the volumetric flowrate and thus of the required pipe diameter. In this paper, the required length is assumed equal to the sum of: (i) the length of roads in the area of consideration, calculated using the Generalised Land Use Database (GLUD) [31], which provides road lengths for different areas of the UK; and (ii) an additional service pipe length depending on the type of dwelling [32]. The design volumetric flowrate $\dot{V}_{\mathrm{DH,des}}$ is determined based on the peak heat demand of the year:

$$\dot{V}_{\mathrm{DH,des}} = \frac{\dot{Q}_{\mathrm{DH,des}}}{\rho_{\mathrm{w}} c_{\mathrm{p,w}} (T_{\mathrm{DH,flow}} - T_{\mathrm{DH,return}})} \,, \tag{4}$$

where, for the design point denoted with the subscript des, $\dot{Q}_{\mathrm{DH,des}}$ is the peak DH network heat demand. $T_{\mathrm{DH,flow}}$ and $T_{\mathrm{DH,return}}$ are the DH network flow and return temperature, respectively. The water density, ρ_{w}, and specific heat capacity, $c_{\mathrm{p,w}}$, are calculated at the mean bulk temperature (*i.e.*, the average between the flow and return temperatures). The velocity of water through the network pipe v_{DH} depends on the pipe diameter D_{pipe}:

$$v_{DH,\mathrm{des}} = \frac{4\dot{V}_{\mathrm{DH,des}}}{\pi {D_{\mathrm{pipe}}}^2} \,. \tag{5}$$

The maximum allowable flow velocity in the network, $v_{\mathrm{DH,max}}$, is a function of the pipe diameter D_{pipe}, as demonstrated by Delangle *et al.* [25]. A simple optimisation problem is solved to obtain the minimum diameter that satisfies the maximum velocity constraint:

$$\min \{D_{\mathrm{pipe}}\} \,, \tag{6}$$

subject to:

$$v_{DH,\mathrm{des}} < v_{\mathrm{DH,max}} \,. \tag{7}$$

The total installation cost for the DH network, C_{DH}, is calculated using:

$$C_{\mathrm{DH}} = \left(a_{\mathrm{DH,cost}} D_{\mathrm{pipe}} + \beta_{\mathrm{DH,cost}}\right) l_{\mathrm{DH}} \,, \tag{8}$$

where l_{DH} is the DH network length and $a_{\mathrm{DH,cost}}$ and $\beta_{\mathrm{DH,cost}}$ are constants for the estimated cost per m as obtained from the collected cost data. Similarly, the DH network loss, $\dot{Q}_{\mathrm{DH,loss}}$, is obtained from:

$$\dot{Q}_{\mathrm{DH,loss}} = \left(a_{\mathrm{DH,loss}} D_{\mathrm{pipe}} + \beta_{\mathrm{DH,loss}}\right) l_{\mathrm{DH}} \,, \tag{9}$$

where $a_{\mathrm{DH,loss}}$ and $\beta_{\mathrm{DH,loss}}$ are constants for the estimated heat loss per metre as obtained from the collected data. Since the loss from the pipes raises the peak heat demand, the process described by Eqs. (4)-(9) is solved iteratively.

2.1.3. Evaluation of pathway cost and environmental indicators

The objective function to be minimised is the total annualised energy cost, $C_{\mathrm{tot,ann}}$, which includes all annualised capital expenditures (CAPEX) $C_{\mathrm{cap,ann}}$ and operating expenses (OPEX) $C_{\mathrm{op,ann}}$ of installed technology and network; the annual cost of importing electricity, $C_{\mathrm{el,ann}}$; the annual revenue from exporting electricity, $R_{\mathrm{el,ann}}$; the annual cost of importing gas, $C_{\mathrm{gas,ann}}$; and the savings acquired from not using the current production unit, $R_{\mathrm{h,ann}}$:

$$C_{\mathrm{tot,ann}} = C_{\mathrm{cap,ann}} + C_{\mathrm{op,ann}} + C_{\mathrm{gas,ann}} + C_{\mathrm{el,ann}} - R_{\mathrm{el,ann}} - R_{\mathrm{h,ann}} \,. \tag{10}$$

The annualised total investment cost, $C_{\mathrm{cap,ann}}$, is calculated using:

$$C_{\mathrm{cap,ann}} = C_{\mathrm{cap}} \frac{r_{\mathrm{d}}}{(1 + r_{\mathrm{d}})(1 - (1 + r_{\mathrm{d}})^{-t_{\mathrm{LT}}}} \,, \tag{11}$$

where r_{d} is the discount rate, t_{LT} is the lifetime of the installed equipment, and C_{cap} is defined as:

$$C_{\mathrm{cap}} = \sum_j C_j \dot{Q}_{\mathrm{pr,max},j} N_j + C_{\mathrm{DH}}\,, \tag{12}$$

where C_j represents the specific investment cost of each technology j; and C_{DH} is the DH network investment cost (if present in the investigated scenario).

The annual operation and maintenance cost, $C_{\mathrm{op,ann}}$, is calculated as:

$$C_{\mathrm{op,ann}} = \sum_j k_{\mathrm{OM},j} C_j \dot{Q}_{\mathrm{pr,max},j} N_j + k_{\mathrm{OM,DH}} C_{\mathrm{DH}}\,, \tag{13}$$

where $k_{\mathrm{OM},j}$ and $k_{\mathrm{OM,DH}}$ represent the operation and maintenance cost of each technology and the DH network as fractions of their investment costs, respectively.

The cost of importing natural gas, the cost of importing electricity and the revenue from exporting electricity are represented by Eqs. (14)-(16), respectively:

$$C_{\mathrm{gas,ann}} = P_{\mathrm{gas}} \int_{\mathrm{year}} E_{\mathrm{gas}}\ \mathrm{d}t\,, \tag{14}$$

$$C_{\mathrm{el,ann}} = \int_{\mathrm{year}} P_{\mathrm{PE}} E_{\mathrm{PE}}\ \mathrm{d}t\,, \tag{15}$$

$$R_{\mathrm{el,ann}} = \int_{\mathrm{year}} P_{\mathrm{EE}} E_{\mathrm{EE}}\ \mathrm{d}t\,, \tag{16}$$

where P_{gas} is the natural gas price (constant through the year); E_{gas} the time-resolved gas consumption; P_{PE} and P_{EE} are the time-resolved prices of purchasing and exporting electricity, respectively; and E_{PE} and E_{EE} the time-resolved amounts of electricity purchased and exported, respectively.

The savings acquired from not using the current production (natural gas boiler) are equal to:

$$R_{\mathrm{h,ann}} = \frac{P_{\mathrm{gas}}}{\eta_{\mathrm{boil}}} \int_{\mathrm{year}} \dot{Q}_{\mathrm{pr},j}\ \mathrm{d}t\,, \tag{17}$$

where η_{boil} represents boiler efficiency.

For each pathway, the levelised cost of heat (LCOH), C_{LCOH}, is defined as the ratio of the annualised cost of producing heat to the annual heat production:

$$C_{\mathrm{LCOH}} = \frac{C_{\mathrm{cap,ann}} + C_{\mathrm{op,ann}} + C_{\mathrm{gas,ann}} + C_{\mathrm{el,ann}} - R_{\mathrm{el,ann}}}{\int_{\mathrm{year}} \dot{Q}_{\mathfrak{D}}\ \mathrm{d}t}\,. \tag{18}$$

The annual savings, $C_{\mathrm{sav,ann}}$, are determined using:

$$C_{\mathrm{sav,ann}} = R_{\mathrm{el,ann}} + R_{\mathrm{h,ann}} - C_{\mathrm{op,ann}} - C_{\mathrm{gas,ann}} - C_{\mathrm{el,ann}}\,. \tag{19}$$

The payback time, t_{PBT}, is also calculated using:

$$t_{\mathrm{PBT}} = \frac{C_{\mathrm{cap,ann}}}{R_{\mathrm{el,ann}} + R_{\mathrm{h,ann}} - C_{\mathrm{op,ann}} + C_{\mathrm{gas,ann}} + C_{\mathrm{el,ann}}}\,. \tag{20}$$

The CO_2-equivalent emissions, $\mathcal{E}_{\mathrm{CO_2}}$, of each pathway are determined using:

$$\mathcal{E}_{\mathrm{CO_2}} = k_{\mathrm{CF,gas}} E_{\mathrm{gas}} + \int_{\mathrm{year}} k_{\mathrm{CF,grid}} \left(\dot{W}_{\mathrm{grid,imp}} - \dot{W}_{\mathrm{grid,exp}} \right) \mathrm{d}t \,, \tag{21}$$

where $k_{\mathrm{CF,gas}}$ is the carbon footprint factor of natural gas; $k_{\mathrm{CF,grid}}$ the hourly carbon footprint factor of electricity; and $(\dot{W}_{\mathrm{grid,imp}} - \dot{W}_{\mathrm{grid,exp}})$ the power exchanged with the grid. The CO_2-equivalent savings, $\mathcal{E}_{\mathrm{sav,CO_2}}$, compared to the case in which all demand is met by natural gas boilers, thus equal:

$$\mathcal{E}_{\mathrm{sav,CO_2}} = \frac{k_{\mathrm{CF,gas}}}{\eta_{\mathrm{boil}}} \int_{\mathrm{year}} \dot{Q}_{\mathfrak{D}} \, \mathrm{d}t - \mathcal{E}_{\mathrm{CO_2}} \,. \tag{22}$$

2.2. Technoeconomic models

This section presents an analysis of the data collected for commercially available CHP systems, heat pumps, heat-pump compatible hot water cylinders and district heating pipes on the UK market.

2.2.1. Data-driven models from analysis of commercially available products on the UK market

A CHP system is made of two main components: the prime mover, which is connected to a generator to produce electricity, and the heat recovery module, which collects waste heat and transfers it to water for hot water or space heating purposes. Recovering heat from the exhaust gases and jacket water of ICEs is the most-studied option [33,34] for electricity and heat cogeneration. The electricity generated from CHP systems can be used to either meet electrical demand or can be sold back to the grid, producing revenues. Due to the high total efficiency of CHP systems (>85%), reductions in CO_2-equivalent emissions can be expected compared to boiler-only systems. The cost effectiveness of such systems is dependent on the relative price of gas and electricity. In the UK, where the price of electricity is high, CHP systems show significant savings potential [35]. In order to account for the variation of electrical and thermal efficiencies of ICE-CHP systems for different sizes and part-load conditions, information has been collected from more than 15 UK suppliers of more than 150 ICE-CHP units, ranging from small (1 kW_e) to large scale (8 MW_e).

Emission reductions are shown to be very high when heat pumps are integrated in the UK heating network [36]. In their simplest form, heat pumps are made of four main components: an evaporator, a compressor, a condenser, and an expansion valve. Their performance is measured through the coefficient of performance (COP), which is the ratio between the heat output and the power input. The smaller the temperature difference between the heat source and the heat sink, the higher the COP. Due to its low thermal diffusivity, the ground temperature temporal profile throughout the year is more stable than that of the atmospheric air, which is the main reason why GSHPs exhibit higher efficiencies than ASHPs during winter, when heat demand is high. Furthermore, ASHPs often suffer from ice build-up, which requires defrost cycles and therefore additional electricity consumption [37]. In domestic applications, it is necessary that hot water is stored at a minimum temperature of 55 °C, so that the build-up of harmful bacteria is prevented [38]. The characteristics of more than 200 currently advertised ASHPs and GSHPs have been recorded from more than 20 UK suppliers.

Approximate costs and heat loss estimations were also collected for DH network pipes, as well as heat-pump compatible small and medium-scale hot water cylinders.

The information gathered is used to develop data-driven models. KPIs are correlated against technology-specific parameters (*e.g.*, size, heating duty/rating) and operating conditions (*e.g.*, atmospheric air temperature), when available. This allows us not only to capture the cost and performance variability, but also to quantify the uncertainty associated with each indicator, and determine how it propagates through the pathway identification. The indicators thus obtained are reported with 95% confidence intervals, computed from statistical analysis [39].

2.2.1.1. Internal combustion engine CHP systems

The electrical and thermal efficiencies of different ICE-CHP systems commercially available in the UK are displayed as functions of size and part-load level in Fig. 2. The larger the prime mover of the CHP engine, the higher the electrical efficiency. However, this comes with a simultaneous decrease in thermal efficiency. In part-load operation, the electrical efficiency drops, driving thermal efficiency up. Data have been recorded for a large range of sizes (from 1 kW_e to 8 MW_e). Electrical efficiencies vary from about 25% for very small systems (1 kW_e) to over 42% for large systems (3-8 MW_e). As a result, thermal efficiencies for small systems are as high as 60-70%, while they drop down to less than 50% for large systems. Electrical efficiencies decrease by about 5% when the CHP engines operate at half of the intended capacity, with an equivalent 5% increase in thermal efficiency.

All manufacturer data for CHP engine performance corresponds to just three part-load levels: 50%, 75% and 100%. In order to estimate the average performance between these three levels, two simple two-layer feed-forward neural network fits are developed, also shown in Fig. 2. The networks are trained using the Levenberg-Marquardt back-propagation algorithm [40] and 10 hidden neurons, while 70% of the data points are used for training,15% for model validation and 15% for testing.

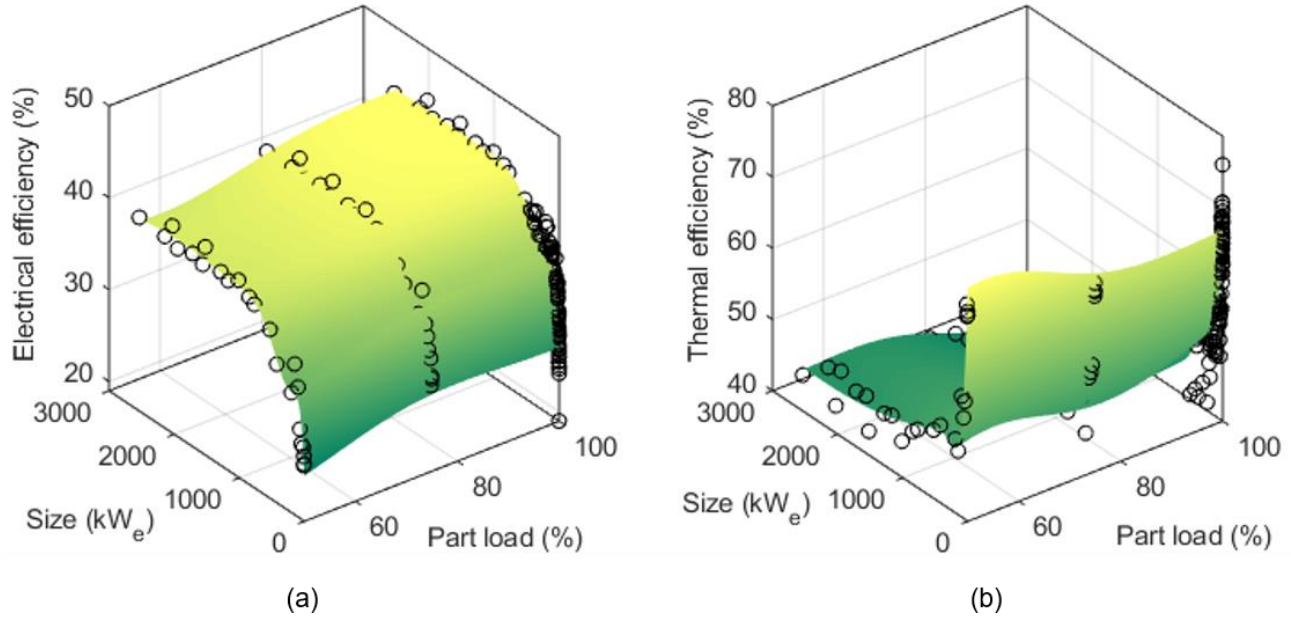


Figure 2. Efficiency of commercially available ICE-CHP systems in the UK as a function of system size and part-load level: (a) electrical efficiency; and (b) thermal efficiency. The plotted data points are extracted from more than 150 manufacturer datasheets and the surfaces represent neural network fits through the data.

The specific cost of CHP systems drops drastically with size. Figure 3 shows the cost and specific cost as a function of size, for sizes up to 800 kW_e.

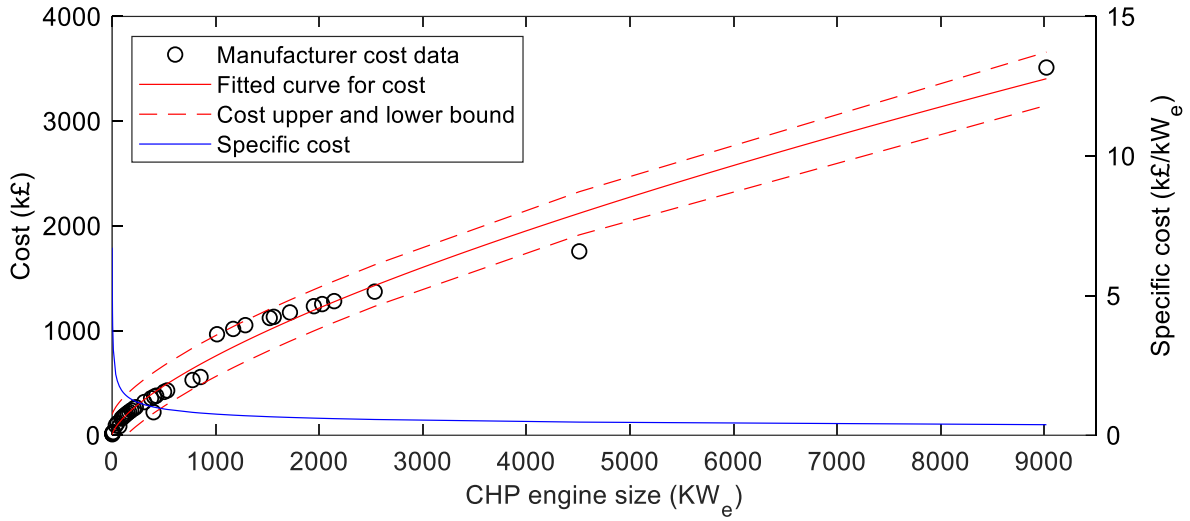


Figure 3. The cost (k£) and specific cost (£/kW_e) of commercially available ICE-CHP systems in the UK as function of system size. Fitted curve and upper/lower prediction bounds appear in red.

2.2.1.2. Air-source and ground-source heat pump systems

The analysis of commercially available ASHPs and GSHPs on the UK market shows that, for the vast majority of residential and commercial applications, single-stage compressors are used to power the vapour compression cycle, using, in more than 80% of the cases, R410a as a working fluid. The latter fluid works at relatively high pressure and is suitable for low-temperature applications, even though it exhibits a high global warming potential (GWP) index, equal to 2088. In recent years, however, many manufacturers tend towards the use of R32, which shows promising performance [41] and has a much lower GWP index of 675 [42]. For GSHPs, both the condenser and the evaporator are brazed-plate heat exchangers (HEXs), while in ASHPs, a plate-fin HEX is used at the air-refrigerant side.

Figure 4 presents the cost and specific cost for different ASHP and GSHP units, as obtained from manufacturers. Unlike the heat pump unit cost, the COP does not change significantly with size for small heat-pump systems and is therefore taken be the same at all considered sizes in this work. On the other hand, the COP of small-size (<10 kW_{th}) ASHP and GSHP units does vary as function of the heat-source (air or ground) temperature, as shown in this figure for a fixed heat-sink temperature (55 °C). All data correspond to monobloc units (single outside units). From the data, it is clear that the cost and COP of ASHPs both show significant variations when comparing values from different manufacturers. For example, the cost of a 7-kW_{th} ASHP ranges between £2000 and £4000, while units of a similar size demonstrate significantly different COP performance.

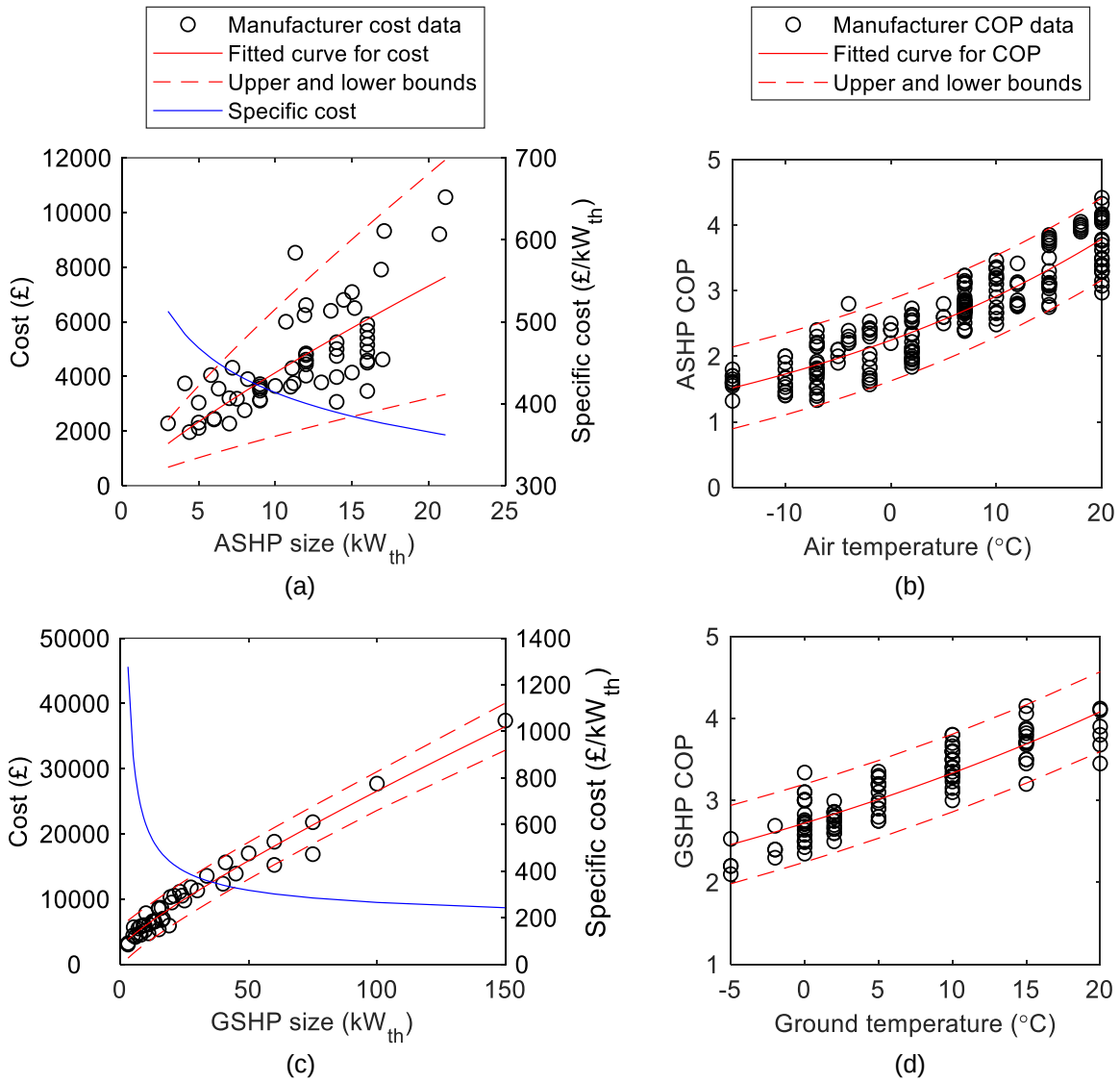


Figure 4. Analysis of commercially available heat pumps on the UK market: (a) cost and specific cost of ASHPs as function of size (rated heat output); (b) COP of ASHPs as function of air temperature; (c) cost and specific cost of GSHPs as function of size (rated heat output); and (d) COP of GSHPs as function of ground temperature. COP-temperature relationships correspond to small sizes (<10 kW_{th}) and a heat sink temperature of 55 °C. Fitted curves and upper/lower prediction bounds appear in red. All data represents monobloc units.

Figure 5 presents the cost and specific cost for small hot water cylinders specifically designed to be integrated with heat pumps. The cost of these units is much higher than typical cylinders and therefore cannot be neglected. An electric heater of about 3-9 kW_{th} is usually incorporated in the cylinder, and if not, this can be usually added at a small cost of about £100 [43]).

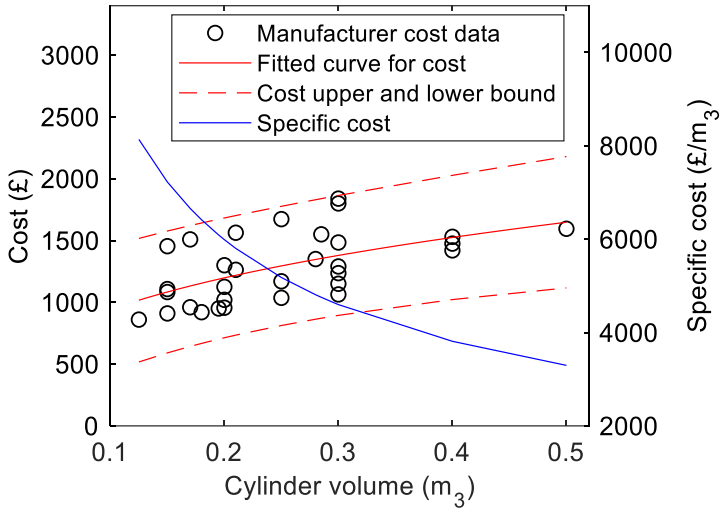


Figure 5. Cost and specific cost of commercially available domestic hot water cylinders as function of size (cylinder volume). Fitted curves and upper/lower prediction bounds appear in red.

2.2.1.3. District heating cost and heat loss

Figure 6 presents the specific cost and heat loss (per unit of pipe length) as functions of the pipe diameter. The cost data involve three different DH projects and are obtained from Ref. [44], while heat loss data are adopted from Ref. [45].

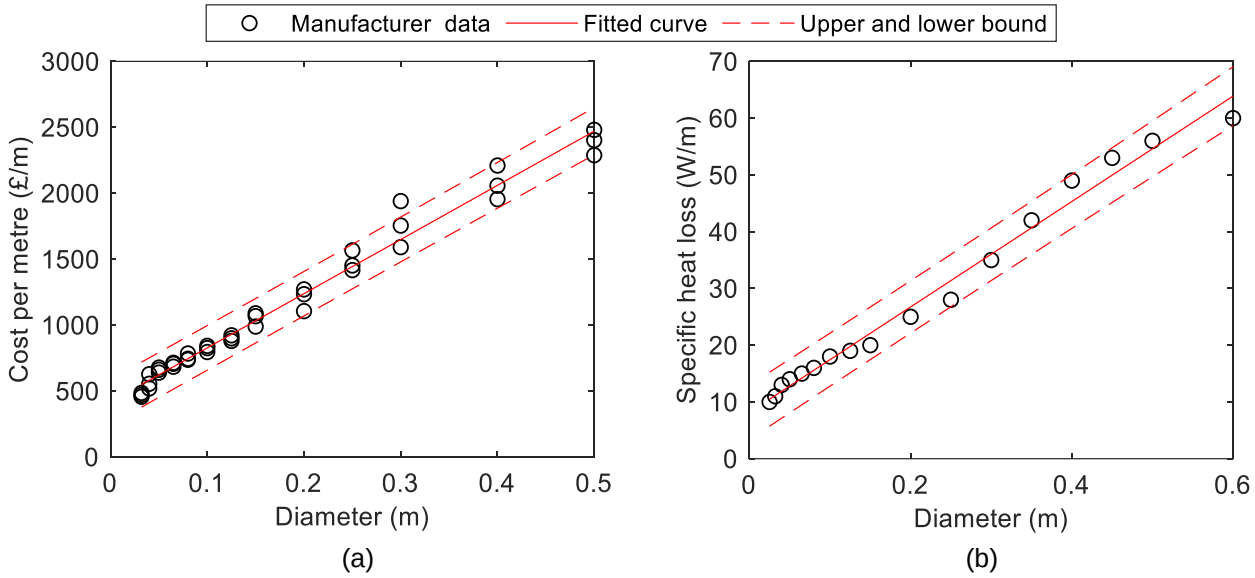


Figure 6. Analysis of data collected for district heating pipes in the UK: (a) specific cost per unit of pipe length; and (b) heat loss per unit of pipe length, as functions of pipe diameter. Data for cost and heat loss acquired from Refs. [44] and [45], respectively.

2.2.1.4. Uncertainty quantification

Table 1 presents a summary of the fits plotted in Section 2 and a quantification of the uncertainty associated to each of the quantities.

Table 1. Models, ranges and uncertainty measures for cost and performance data of CHP systems and heat pumps.

Quantity	Model	Range	Absolute uncertainty*	Relative uncertainty*
CHP systems				
Electrical efficiency (%) of CHP engine as function of part-load level (%) and size (kW_e)	Neural network	$\dot{W}_{\mathrm{el,CHP}} < 8\ \mathrm{MW_e}$ $50\% < \mathrm{PL} < 100\%$	$u_{\eta_{\mathrm{el}}}$ = 2.8% for $\overline{\eta_{\mathrm{el}}}$ = 35%	$\varepsilon_{\eta_{\mathrm{el}}}$ = 8.2% for $\overline{\eta_{\mathrm{el}}}$ = 35%
Thermal efficiency (%) of CHP engine as function of part-load level (%) and size (kW_e)	Neural network	$\dot{W}_{\mathrm{el,CHP}} < 8\ \mathrm{MW_e}$ $50\% < \mathrm{PL} < 100\%$	$u_{\eta_{\mathrm{th}}}$ = 5.9% for $\overline{\eta_{\mathrm{th}}}$ = 55%	$\varepsilon_{\eta_{\mathrm{th}}}$ = 11% for $\overline{\eta_{\mathrm{th}}}$ = 55%
Cost (£) of CHP engine as function of size (kW_e)	$C_{\mathrm{CHP}} = 11000\dot{W}_{\mathrm{el,CHP}}^{\ 0.57}$	$\dot{W}_{\mathrm{el,CHP}} < 8\ \mathrm{MW_e}$	$u_{C_{\mathrm{CHP}}}$ = 200 £ for $\overline{C_{\mathrm{CHP}}}$ = 1.7 k£	$\varepsilon_{C_{\mathrm{CHP}}}$ = 12% for $\overline{C_{\mathrm{CHP}}}$ = 1.7 k£
Heat pump systems				
Cost (£) of ASHPs as function of size (kW_{th})	$C_{\mathrm{ASHP}} = 620\dot{Q}_{\mathrm{ASHP}}^{\ 0.82}$	$\dot{Q}_{\mathrm{ASHP}} < 25\ \mathrm{kW_{th}}$	$u_{\mathrm{C_{ASHP}}}$ = 2.5 k£ for $\overline{C_{\mathrm{ASHP}}}$ = 4.8 k£	$\varepsilon_{\mathrm{C_{ASHP}}}$ = 53% for $\overline{C_{\mathrm{ASHP}}}$ = 4.8 k£
Cost (£) of GSHPs as function of size (kW_{th})	$C_{\mathrm{GSHP}} = 470\dot{Q}_{\mathrm{GSHP}}^{\ 0.85}+2600$	$\dot{Q}_{\mathrm{GSHP}} < 150\ \mathrm{kW_{th}}$	$u_{\mathrm{C_{GSHP}}}$ = 2.9 k£ for $\overline{C_{\mathrm{GSHP}}}$ = 22 k£	$\varepsilon_{\mathrm{C_{GSHP}}}$ = 13% for $\overline{C_{\mathrm{GSHP}}}$ = 22 k£
COP of ASHPs as function of heat source temperature (°C), where heat sink is at 55 °C	$COP = 2.3e^{0.026T_{\mathrm{src}}}$	$\dot{Q}_{\mathrm{ASHP}} < 25\ \mathrm{kW_{th}}$ $-15 < T_{\mathrm{src}} < 20\ °\mathrm{C}$	u_{COP} = 0.6 for $\overline{\mathrm{COP}}$ = 2.4	$\varepsilon_{\mathrm{COP}}$ = 25% for $\overline{\mathrm{COP}}$ = 2.4
COP of GSHPs as function of heat source temperature (°C), where heat sink is at 55 °C	$COP = 2.7e^{0.020T_{\mathrm{src}}}$	$\dot{Q}_{\mathrm{GSHP}} < 25\ \mathrm{kW_{th}}$ $-5 < T_{\mathrm{src}} < 20\ °\mathrm{C}$	u_{COP} = 0.5 for $\overline{\mathrm{COP}}$ = 3.2	$\varepsilon_{\mathrm{COP}}$ = 16% for $\overline{\mathrm{COP}}$ = 3.2
Cost (£) of heat-pump compatible hot water cylinder as function of size (m^3)	$C_{\mathrm{cyl}} = 2100V_{\mathrm{cyl}}^{\ 0.35}$	$V_{\mathrm{cyl}} < 0.6\ \mathrm{m^3}$	$u_{\mathrm{C_{cyl}}}$ = 0.5 k£ for $\overline{C_{\mathrm{cyl}}}$ = 1.4 k£	$\varepsilon_{\mathrm{C_{cyl}}}$ = 35% for $\overline{C_{\mathrm{cyl}}}$ = 1.4 k£
DH network				
Cost per metre of pipe length (£/m) as function of pipe diameter (m)	$C_{\mathrm{DH,sp}} = 4100D_{\mathrm{pipe}} + 420$	$D_{\mathrm{pipe}} < 0.5\ m$	$u_{\mathrm{C_{DH,sp}}}$ = 170 £/m $\overline{\mathrm{C_{DH,sp}}}$ = 1.5 k£/m	$\varepsilon_{\mathrm{C_{DH,sp}}}$ = 11% at $\overline{\mathrm{C_{DH,sp}}}$ = 1.5 k£/m
Heat loss per metre of pipe (W/m) as function of pipe diameter (m)	$\dot{Q}_{\mathrm{DH,loss}} = 93D_{\mathrm{pipe}} + 8.2$	$D_{\mathrm{pipe}} < 0.5\ m$	$u_{\dot{\mathrm{Q}}_{\mathrm{DH,loss}}}$ = 4.6 W/m $\overline{\dot{\mathrm{Q}}_{\mathrm{DH,loss}}}$ = 37 W/m	$\varepsilon_{\dot{\mathrm{Q}}_{\mathrm{DH,loss}}}$ = 12% $\overline{\dot{\mathrm{Q}}_{\mathrm{DH,loss}}}$ = 37 W/m

* Relative and absolute uncertainties are reported at mid-range values (denoted with an overbar ▪).

Table 1 shows that the data-driven models capture the CHP cost and efficiency data with a good accuracy, resulting in low uncertainties (with relative uncertainties below 12% at mid-range values), while the scattering of the available ASHP cost data (see Fig. 4(a)) leads to important deviation and high uncertainties, with a relative uncertainty on the ASHP cost of 53% for a mid-cost heat pump ($\overline{C_{\mathrm{ASHP}}}$ = 4.8 ± 2.5 k£). The latter figure is by far the highest relative uncertainty reported in Table 1,

followed by that on the hot water cylinder ($\varepsilon_{C_{cyl}}$ = 35% for a mid-cost cylinder $\overline{C_{cyl}}$ = 1.4 ± 0.5 k£), the cost of which is however is much lower than that of an ASHP, thus resulting in a less significant absolute uncertainty. It is also worth noting that the relative uncertainty on the ASHP COP is as high as 25%.

The large scattering observed in both the price and performance of ASHPs reflects the fact that a large number of design options exist for these systems (choice of working fluid, size of the heat exchangers, fixed- or variable-speed compressor units, electronic or thermostatic expansion valves, low- or high-noise fans, advanced or simplified controls, defrosting method). In other words, large cost and COP differences are observed between low- and high-specification heat pumps, which explains the high uncertainty obtained with a technology-agnostic approach, whereby the KPIs are correlated against single parameters (*e.g.*, cost as a function of size). In this paper, a refined model of air-source heat pump systems is proposed to enhance the granularity of both the cost and thermodynamic models, so as to reduce the associated uncertainty and capture the full technoeconomic potential of this heat-upgrading technology.

2.2.2. Thermodynamic and costing models of heat pumps

The variation in different ASHP designs and associated cost and performance is large, causing significant uncertainties. Identifying the optimal heat decarbonisation pathways of the future requires reducing these uncertainties, and this can be done through the development of thermodynamic and costing models that can predict some of these variations.

2.2.2.1. Thermodynamic performance model

In the effort to capture design variations and off-design performance of heat pumps, a spatially lumped thermodynamic model of a low-temperature heat pump with a single-stage-compressor is developed. This assumes isenthalpic expansion through the expansion valve, steady-state operation of components and no pressure losses across the pipes and heat exchangers. A schematic of the heat pump cycle is shown in Fig. 7. This involves four main steps: process 1-2 involves the compression of the working fluid; 2-3 the heat rejection to hot water; 3-4 the isenthalpic expansion; and 4-1 the heat addition from the heat source (air, water). The heat pump model utilises compressor efficiency maps adopted from the work of Astolfi [46], providing the isentropic efficiency as a function of volume ratio and volumetric flowrate based on more than 100 Bitzer compressors [47]. The work also utilises comprehensive HEX models, which capture the performance and cost of different HEX designs and can be used to size the HEXs or to predict their performance in off-design conditions. The condenser is a brazed-plate heat exchanger made of three distinct zones: (i) the desuperheating zone (Process 2-2a); (ii) the condensing zone (Process 2a-2b); and (iii) the subcooling zone (Process 2b-3). The evaporator, is either a brazed-plate or a plate-fin heat exchanger, depending on the source (water or air) and involves: (i) the evaporating zone (Process 4-4a); and (ii) the superheating zone (Process 4a-1). The main model equations are listed in Table 2.

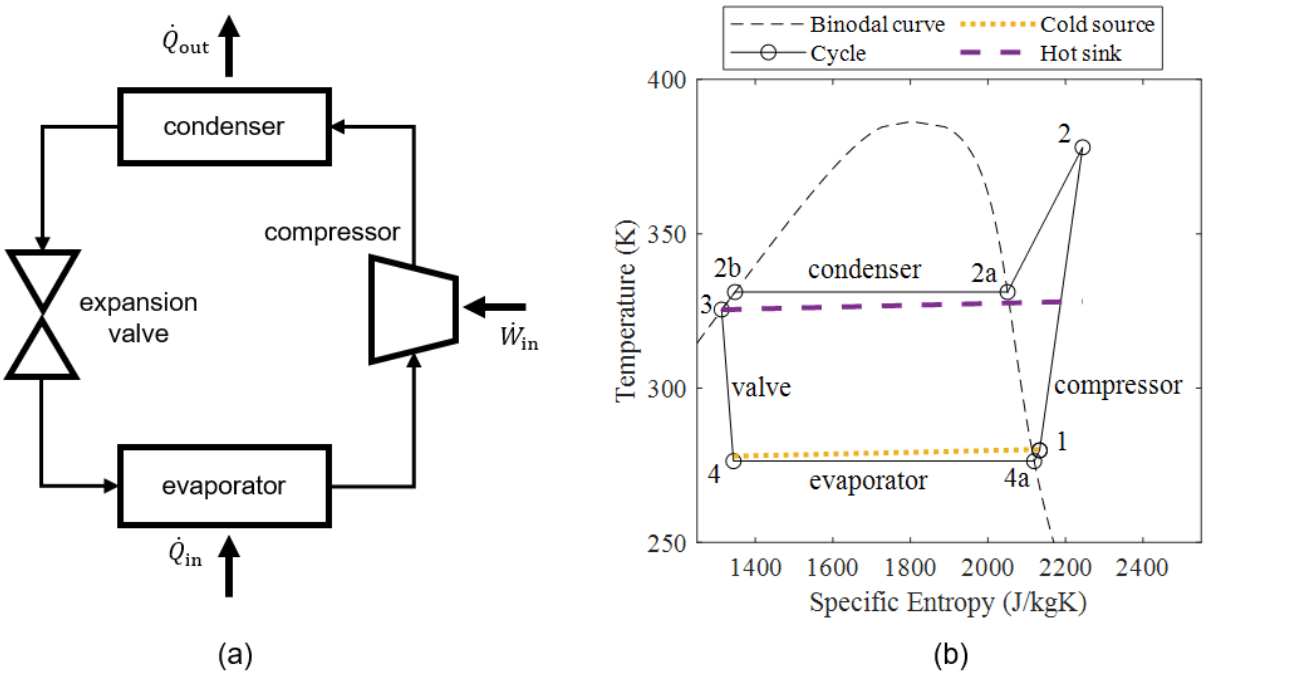


Figure 7. Vapour-compression heat pump cycle: (a) schematic diagram; and (b) *T-s* diagram.

Table 2. Overview of thermodynamic heat pump model. See Nomenclature for symbols.

Piece of equipment	Assumptions	Equations
Compressor	• Well-insulated compressor • Utilises compressor efficiency maps from the work of Astolfi [46]	$h_2 = h_1 + \frac{h_{2,is} - h_1}{\eta_{is,comp}}$ $\eta_{is,comp} = c\left[0.940 + 0.0293\ln\left(\dot{V}_{in}\right) - 0.0266V_r\right]$ $c = 1 - 0.264\ln\left(\frac{V_r}{7}\right)$ for $V_r > 7$, $\dot{W}_{comp} = \dot{m}_{wf}(h_2 - h_1) = \frac{\dot{m}_{wf}(h_{2,is} - h_1)}{\eta_{comp}}$
Condenser	• No pressure drop	$d_{sc} = T_{2b} - T_3$ $\dot{Q}_{out} = \dot{m}_{wf}(h_2 - h_3)$ $\dot{Q}_{out} = \dot{m}_{sink}c_{p,sink}\left(T_{sink,out} - T_{sink,in}\right)$
Expansion valve	• Isenthalpic process	$h_4 = h_3$
Evaporator	• No pressure drop	$d_{sh} = T_1 - T_4$ $\dot{Q}_{in} = \dot{m}_{wf}(h_1 - h_4)$ $\dot{Q}_{in} = \dot{m}_{src}c_{p,src}\left(T_{src,in} - T_{src,out}\right)$

The COP of the heat pump is calculated from:

$$\mathrm{COP} = \frac{\dot{Q}_{in} + \dot{W}_{comp}}{\dot{W}_{comp}}. \tag{23}$$

The heat pump modelling effort involves two optimisation parts. The first task is the design optimisation problem, where for nominal source and sink conditions, the evaporation pressure P_{evap}, the condenser pressure P_{cond}, the degree of superheating d_{sh} and the degree of subcooling d_{sc} are optimised to maximise the heat pump's COP, as shown in Eq. (24). In this stage, a minimum temperature difference

is defined between heat exchanger fluids, known as the pinch-point temperature difference (PPTD). Large PPTDs mean small HEXs and subsequently low COPs and low costs. Small PPTDs, on the other hand, mean high COPs but increased costs. It is important to state that dry air is assumed in this work to enter the evaporator. Details on HEX modelling and validation of the assumption of dry air appear Appendix A. The heat pumps are designed following the optimisation problem:

$$\max_{P_{\text{evap}}, P_{\text{cond}}, d_{\text{SC}}, d_{\text{SH}}} \{\text{COP}\}, \tag{24}$$

and following this design, all HEXs are first sized and then costed as per Section 2.2.2.2.

The second task involves the off-design operation optimisation problem, where for a varying heat-source temperature and fixed HEX size, the COP is again maximised, assuming that an electronic expansion valve can be used to control the degree of superheating d_{sh} and a variable-speed compressor to control the working fluid mass flow rate $\dot{m}_{\text{wf}}$, as shown in Eq. (25):

$$\max_{\dot{m}_{\text{wf}}, d_{\text{SH}}} \{\text{COP}\}. \tag{25}$$

2.2.2.2. Costing

Assigning costs to different heat pump components happens utilising cost correlations as acquired by: (i) Freeman *et al.* [48] for water pump and compressor; (ii) Lecompte *et al.* [49] for air fan and plate-fin HEX; (iii) Carel [50] for expansion valve; and (iv) DECC [51] for miscellaneous hardware costs and profit margins. All correlations are adjusted to GBP (£) and based on inflation, according to the Chemical Engineering Plant Cost Index (CEPCI) [52] and are listed in Appendix B.

2.2.2.3. Model validation

The heat pump thermodynamic model is validated by comparing model predictions to cost and performance data of two commercially available ASHP monobloc systems: Ecodan (Mitsubishi Electric) [53] and Aquarea H-generation (Panasonic) [54]. The two systems share similar size ranges (5-14 kW_{th} and 5-16 kW_{th} respectively), same refrigerant (R410a), same operation range (-20-35 °C), variable-speed compressor, similar sound levels (46-53 dB and 49-54 dB respectively) and same energy efficiency class (A++). In the validation process, the PPTD is set to 5 °C. Figure 8(a) illustrates the COP as a function of air temperature for a heat sink temperature of 55 °C, as recorded by the two systems' datasheets and as predicted by the thermodynamic model. Figure 8(b) compares cost data of the two heat pump systems to model predictions. The mean relative uncertainty of the COP and cost predictions are calculated to be 11.0% and 9.3%, respectively.

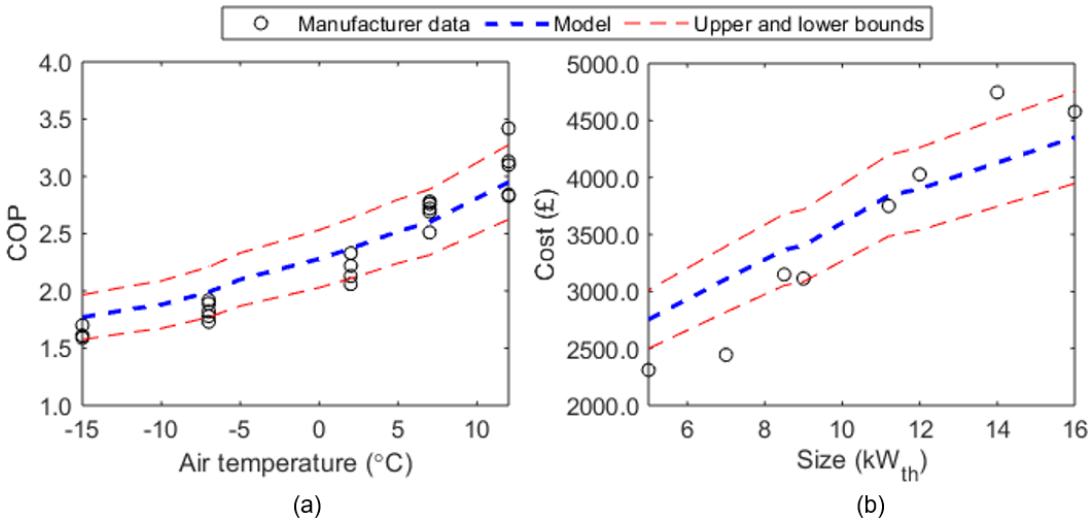


Figure 8. Comparison of heat pump thermodynamic model predictions to manufacturer data for: (a) COP as a function of air temperature (heat sink = 55 °C); and (b) specific cost as a function of size (rated heat output).

3. Case Study: The Isle of Dogs, London

The feasibility study and comparison of centralised and distributed heating options is conducted for the case of Isle of Dogs, a highly populated area in East London, UK. According to mid-2018 population estimates, it is estimated to have a population of about 58000 people, which corresponds to 19475 households and a total of 1050 buildings [55]. The area covered by the Isle of Dogs is obtained using the socio-economic data for different MSOAs collected in 2013 [56] to be about 23 km^2 and the road length is estimated according to GLUD [31]. The model utilises hourly space heating and hot water demand profiles. The profiles have been obtained from the agent-based model developed in project "EDF Flexifund", a collaboration between Imperial College London and EDF Energy [57]. This involved collecting data for the Isle of Dogs' area layout, building types (age, height, comfort temperature, floorspace, *etc.*), household size, economic activity, daily temperature profiles and road network. Electricity and heat demands were simulated using computer representations of decisions makers and were validated based on benchmark data published by DECC [58, 59]. Figure 9 illustrates the region's middle-layer super output areas (MSOAs), as well as the demand profiles for hot water and space heating for 12 typical days of the year during 2014. The peak domestic heat demand reaches 81 MW.

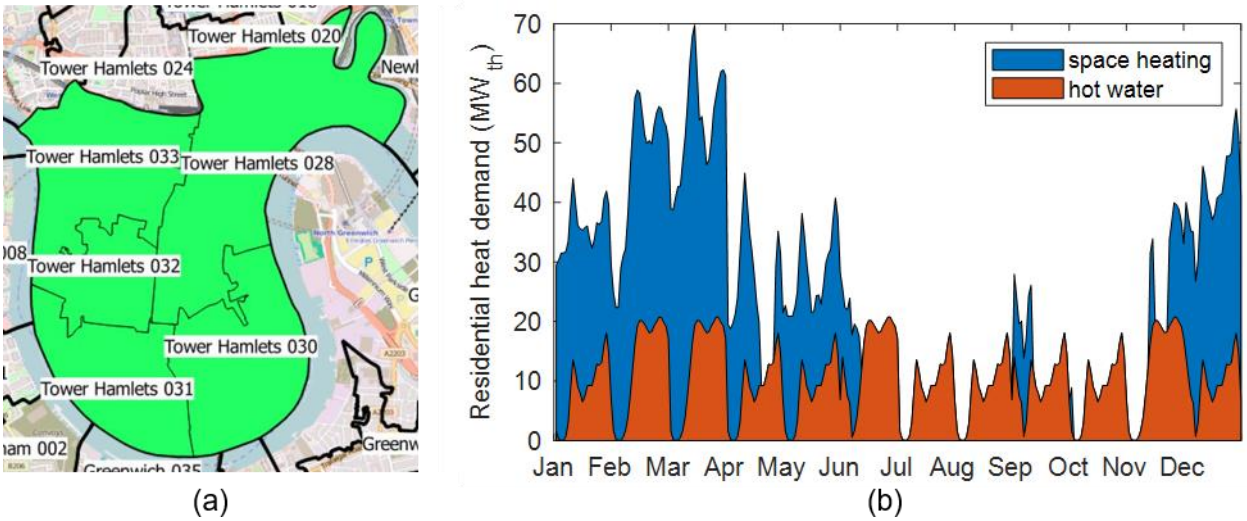


Figure 9. Isle of Dogs area in London: (a) five MSOAs that compose the region; and (b) residential space heating and hot water demand for 12 typical days of the year.

3.1. Model inputs and assumptions

Main model assumptions and inputs are listed below:

- In the energy-community pathway, it is assumed that each energy community is composed by 19 households (the group of households that correspond to the average building of the region.
- In all pathways concerning heat pumps, it is assumed that heat pumps should provide heat for both space heating and hot water (heat sink temperature of 55 °C).
- The specific investment cost of backup large-scale boilers is assumed to be 40 £/kW_{th} (average of the cost of more than 20 units larger than 1 MW_{th} [60]), while that of medium-scale backup boilers in the case different CHP systems are installed in each energy community is assumed equal to 50 £/kW_{th}, (average of the cost of more than 30 units in the range of 50-150 kW_{th} [60]).
- The specific cost for large-scale (>1 MWh_{th}) and medium-scale (50-150 kW_{th}) hot water storage is 960 £/m^3 [36] and £2000 (from collected cost data) respectively.
- In the case of CHP systems, it is assumed that installation adds 20% to the investment cost [61].
- The minimum part-load level at which the CHP systems can operate is set to 50% [62].
- In the centralised system pathway, the specific cost of CHP systems is assumed to remain constant for sizes >8 MW_e (engines are stacked up).

- The cost required for the installation of small-scale ASHP units is set at 20% of the investment cost, which is in line with DECC [51]. GSHPs are more expensive due to the requirement to lay ground pipes; an additional cost of 650 £/kW_{th} is assumed [63].
- The air is assumed to be dry (see Section 2.2.2.1), while the ground temperature is assumed not to change over time. The validity of the former assumption is considered in Appendix A, and a sensitivity analysis to explore the validity of latter assumption is conducted in Section 3.2.1.
- According to the CIBSE's heat network code of practise [64, 65], pipework sizing is performed for flow and return temperatures of 90 °C and 60 °C Although this does not take into account flow and return temperatures of each building, ignoring the potential to reduce temperature differences during the summer, it is considered safer to slightly overestimate requirements to ensure the network's reliability at all times of the year [65].
- The capital cost is annualised for a technology lifetime of 20 years [36] and a discount rate of 5%.
- The price of gas is set at 0.04 £/kWh [36], while hourly importing and exporting electricity prices are obtained from Nord Pool in 2019 [66] and by breaking down electricity costs into components as explained in the work of Acha *et al.* [67] (average importing electricity price is 0.14 £/kWh).
- The carbon footprint of natural gas is set at 0.18 $kgCO_{2(eq)}$/kWh [68], while annual hourly data for the carbon footprint of the grid is obtained from the National Grid in 2020 [69] (average grid carbon footprint is 0.22 $kgCO_{2(eq)}$/kWh).

The annual fluctuation of COP for average-performance ASHP and GSHP units is shown in Fig. 10. The result shown in this figure is based on the data-driven models of heat pumps for a heat sink temperature of 55 °C and the mean daily air and ground temperatures as recorded in London, UK, in 2014 [70]. GSHPs show a more stable performance with the COP remaining close to 3, while the COP of ASHPs varies from about 2 in the winter to more than 4 in the summer.

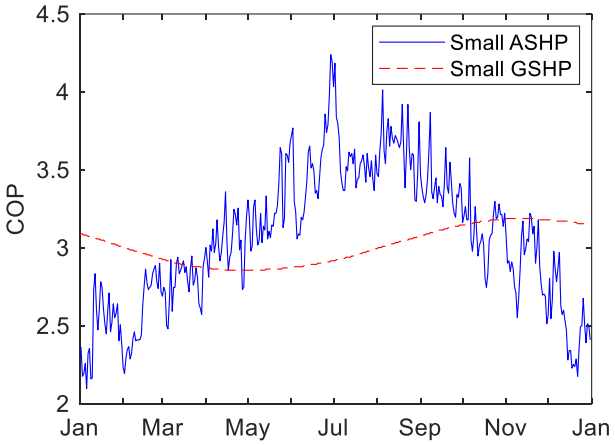


Figure 10. Annual fluctuation of COP of average-performance ASHP and GSHP units utilising air and ground temperature measurements in London, UK, in 2014 [70].

3.2. Comparison of pathways based on data-driven models

For each pathway, the optimisation problem provides an optimal technology size that minimises the total annualised energy cost $C_{\mathrm{tot,ann}}$. As an example, Fig. 11 presents how the optimally sized technology and its backup system work simultaneously to meet heat demand for two of the pathways: (i) centralised CHP system and backup boiler; and (ii) domestic ASHP systems and backup electric heaters, for 12 typical days of the year.

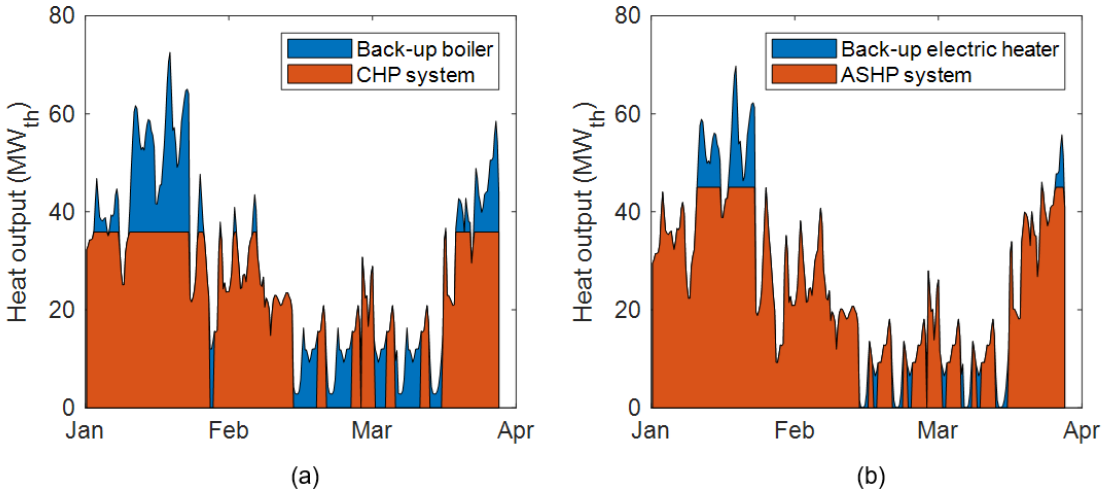


Figure 11. Division of duty between main heat generation technology and backup system for: (a) centralised CHP system and backup boiler; and (b) domestic ASHP system and backup electric heater.

As shown in Fig. 11, when the demand is higher than the capacity of the heat generation technology, backup systems provide the additional required heat. Similarly, when the demand is lower than the minimum capacity of the system, the latter is switched-off and backup systems meet the demand instead. The main results of the comparison of possible pathways are presented in Table 3. Annual savings S_{ann} correspond to savings compared to the case in which all heat demand covered by decentralised boilers (current production unit).

Table 3. Comparison of heat generation pathways in terms of: optimal technology size, backup requirement, levelised cost of heat C_{LCOH}, total annualised energy cost $C_{\mathrm{tot,ann}}$, investment cost $C_{\mathrm{cap,ann}}$, savings $C_{\mathrm{sav,ann}}$, payback period t_{PBT} and CO_2-equivalent emission savings $\mathcal{E}_{\mathrm{sav,CO_2}}$. Energy communities correspond to 19 households.

Quantity	Optimal size (kW_{th})	Backup capacity (kW_{th})	C_{LCOH} (£/MWh_{th})	$C_{\mathrm{tot,ann}}$ (M£)	$C_{\mathrm{cap,ann}}$ (M£)	$C_{\mathrm{sav,ann}}$ (M£)	t_{PBT} (years)	$\mathcal{E}_{\mathrm{sav,CO_2}}$ (%)
Centralised CHP system	35000	48000 (boiler)	31	-3.8	150	13	12	-1.3
CHP systems in energy communities	32	48 (boiler)	52	1.7	133	6.4	21	4.0
Micro-CHP systems at household level	0.7	4.1 (boiler)	50	1.0	68	3.2	21	5.6
GSHP systems in energy communities	44	36 (electric heater)	74	7.0	99	-0.9	-	60
Domestic ASHP systems	3	2.8 (electric heater)	72	6.1	53	-2.9	-	55
Domestic GSHP systems	3	2.8 (electric heater)	79	8.0	108	-1.3	-	62

In order to capture the effect of scale on the possible decarbonisation pathways, simulations are conducted for varying technology size and Fig. 12 demonstrates how the LCOH, the total investment cost, the annual savings and the CO_2-equivalent savings compare between the different options. On the *x*-axis, the size is normalised with respect to the peak heat demand.

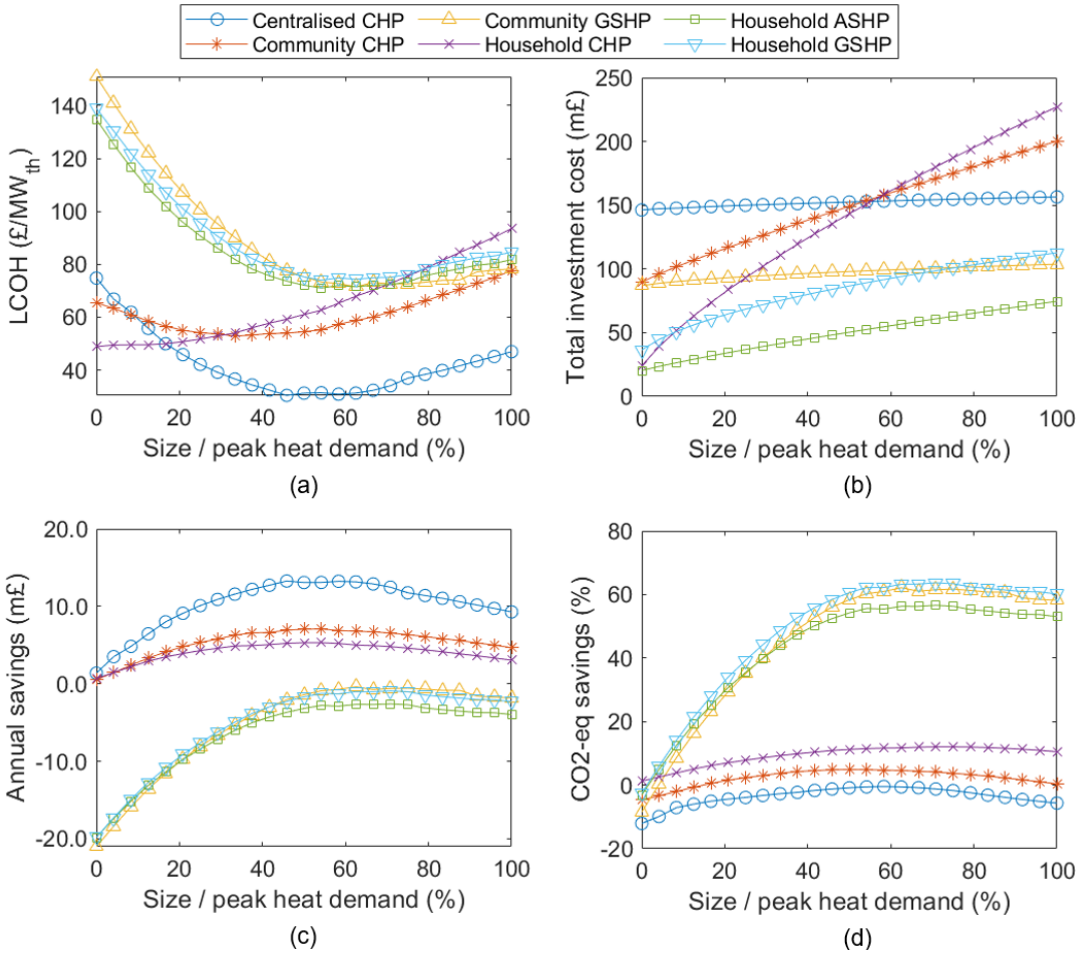


Figure 12. Comparison of heat generation pathways in terms of: (a) LCOH; (b) total investment cost; (c) annual profit; (d) CO_2-equivalent savings, for varying technology size. The latter is normalised to peak heat demand.

The centralised CHP system requires a significant investment cost (£150M), which is higher than all other options, due to the significant cost of the DH network (85% of the investment cost). However, as shown in Fig. 12(c), the CHP system shows higher annual savings than all other pathways at all sizes. This is attributed to the high electrical efficiency of large CHP systems and therefore the ability to sell significant amounts of electricity to the grid. Despite the high investment cost, the centralised ICE-CHP pathway appears to be the least-cost pathway at almost all sizes. The optimal size is about 35 MW_{th}, which corresponds to a LCOH of 31 £/MWh_{th} (Table 3) and a PBT of 12 years, showing that the centralised ICE-CHP system is the most cost-effective investment. It is clear from Fig. 12 that the effect of size is particularly important in the value of the system, since a centralised CHP system designed to supply 100% of the peak demand would result to a LCOH of 47 £/MWh_{th}, which would be significantly higher than the LCOH of the optimally sized system.

CHP systems installed in energy communities and micro-CHP systems at each household show very similar performance, achieving an LCOH of 52 £/MWh_{th} and 50 £/MWh_{th} respectively, while they both achieve a PBT of about 21 years. These systems experience lower electrical efficiency than the centralised system, therefore annual savings are significantly lower (Fig. 12(c)). Micro-CHP systems experience high specific costs and show not to compete to centralised systems, while when sized to meet the peak heat demand, they show higher prices than heat pumps (Fig. 12(b)).

The pathways considering ASHPs and GSHPs show a LCOH higher than 70 £/MWh_{th} (Fig. 12(a)), which makes them a more expensive heat generation solution than CHP systems. GSHPs installed at household level show significantly higher investment costs than ASHPs, however they achieve very similar performance in terms of LCOH. As shown in Table 3, the main drawback of heat pump

systems is that they exhibit negative annual savings, attributed to the fact that the total cost of buying electricity to run the heat pumps is almost always higher than the cost of fuel required in boilers. This is explained by the significant difference in the price of natural gas and electricity in the UK, with the first being about 4 times lower than the average importing electricity price in 2020 [66].

Although cost analysis shows that a centralised CHP system is the least-cost pathway, it is very important to observe the degree of decarbonisation achieved in each pathway. ICE-CHP systems recover heat from ICEs that would be otherwise wasted, achieving total efficiencies close to 90%, therefore one would assume significant emission reductions. However, in recent years, the carbon footprint of the electricity from the grid is significantly decreasing, having dropped from about 0.50 $kgCO_{2(eq)}$/kWh in 2014 to an average of 0.22 $kgCO_{2(eq)}$/kWh in 2020 [71]. This is very close to the carbon footprint of natural gas (0.18 $kgCO_{2(eq)}$/kWh), which means that emissions from ICE-CHP systems are similar to those of boilers. In detail, centralised CHP systems show negative emission savings (-1.3%), which means that, at the moment, these are not viable options to decarbonise the heat sector. Although the higher thermal efficiency of smaller micro-CHP systems provides positive emission savings, these are less significant (5.6%).

Unlike gas-fired CHP systems, heat pumps are becoming an increasingly promising heat decarbonisation solution. As shown in Table 3, the use of GSHPs, either at household or energy-community level, can provide CO_2-equivalent savings of at least 60%. Similarly, domestic ASHPs demonstrate CO_2-equivalent savings of 55%, while the LCOH is 72 £/MWh_{th}, just below that of GSHPs installed at energy-community level (74 £/MWh_{th}). The main advantage of ASHPs compared to GSHPs is that they involve significantly lower capital cost (£53M).

In this work, the inlet source (ground) temperature has been assumed to remain constant throughout the year. Heat extraction from the ground over a significant amount of time can cause the temperature of the soil to reduce over time, reducing the heat pump COP and increasing operational costs in the long run. The degree to which the heat extracted from the soil is higher than that injected into the soil depends on various factors, including the density of GSHP installations, weather, as well as possibilities of heat gain from other sources. In central London, there are multiple sources of heat gain, including solar and human activity (associated with the so-called urban heat-island effect) related gains, gains from the waste-water and sewer systems, heat generated by significant underground train traffic, as well as the fact that the Isle of Dogs area is surrounded by the Thames river whose water will act as a thermal source in winter when the soil temperature drops while the water temperature remains more steady. Nevertheless, we consider here an “extreme” case which re-evaluates results concerning the utilisation of GSHPs assuming that there are no heat gains from other sources and that the ground temperature reduces by ~0.5 °C every year, consistent with Refs. [72–74] for soil temperature decreases in cold regions attributed to the fact that heat is extracted from the soil all year round. Results are shown in Table 4.

Table 4. Comparison of GSHP pathways in terms of levelised cost of heat C_{LCOH}, total annualised energy cost $C_{\mathrm{tot,ann}}$ and savings $C_{\mathrm{sav,ann}}$, assuming an annual reduction of ~0.5 °C in ground temperature.

Quantity	C_{LCOH} (£/MWh_{th})	$C_{\mathrm{tot,ann}}$ (M£)	$C_{\mathrm{sav,ann}}$ (M£)
GSHP systems in energy communities	78	8.1	-1.9
Domestic GSHP systems	84	9.2	-2.8

As demonstrated in Table 4, the worst-case effect of soil thermal imbalance, in the absence of heat gains from any sources, is to cause an increase of ~5% and ~6% in the LCOH of GSHP systems

installed in communities or at domestic level, respectively. Although accounting for this variation will not appreciably change the present results, it would be necessary to consider solutions to deal with any thermal imbalance in a pathway dominated by rapid employment of GSHPs, including design considerations (borehole space and length, soil water content, auxiliary energy sources, *etc.* [72]).

3.3. Comprehensive prediction of ASHP potential

The overall annualised energy cost and carbon emissions of alternative pathways may change when different cost and performance assumptions apply. Especially in the case of ASHPs, which have shown a very large uncertainty in the capital cost (Table 1, Section 2.2.1), it is necessary to capture interactions between the multi-process components. In this effort, the thermodynamic heat pump model is used to differentiate between two possible heat pump designs: (i) a high-specification heat pump that utilises large heat exchangers (corresponding to a PPTD of 1 °C) and operates with R32 as the working fluid; and (ii) a low-specification heat pump that utilises small heat exchangers (corresponding to a PPTD of 10 °C) and operates with R410a as the working fluid. The design optimisation problem is solved to size the components at a design point chosen at: (i) a heat source temperature of 7 °C (industrial standard for quoting ASHP efficiency [75]); and (ii) a heat-sink temperature of 55 °C, which is the minimum required for hot water [38]. The associated component costs are determined and the off-design COP variation with temperature is obtained, assuming that both heat pumps involve an electronic expansion valve and a variable-speed compressor. Figure 13 shows the specific cost of the two heat pump designs as function of size and their off-design performance for varying air temperature. The latter does not change significantly with size for small systems and is therefore assumed to be the same at all considered sizes.

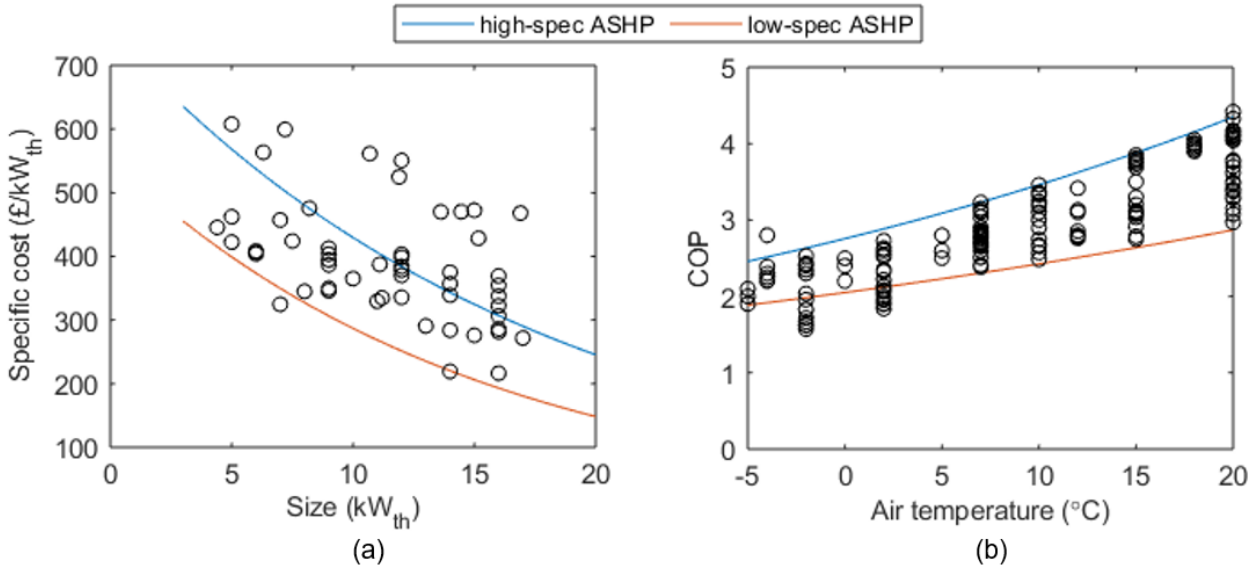


Figure 13. Thermodynamic model predictions against manufacturer data: (a) specific cost as function of size; and (b) COP as function of air temperature (for a heat sink temperature of 55 °C), for the cases of a high-specification ASHP with large heat exchangers and working fluid R32; and a low-specification ASHP with small heat exchangers and working fluid R410a. Small circles represent collected data.

Figure 13 demonstrates that the predicted cost and performance of the two heat pump designs could indeed represent a high-spec and a low-spec heat pump on the UK market. The high-spec option exhibits a high cost but a favourable performance, while the low-spec one has a lower cost but lower performance. The results of the comparison of the two designs when used to provide heating for each household in the Isle of Dogs are shown in Table 5 and Fig. 14.

Table 5. Comparison of two ASHP pathways in terms of: optimal technology size, backup requirement, levelised cost of heat C_{LCOH}, total annualised energy cost $C_{\mathrm{tot,ann}}$, investment cost $C_{\mathrm{cap,ann}}$, savings $C_{\mathrm{sav,ann}}$, payback period t_{PBT} and CO2-equivalent emission savings $\mathcal{E}_{\mathrm{sav,CO_2}}$.

Quantity	Optimal size (kW_{th})	Backup capacity (kW_{th})	C_{LCOH} (£/MWh_{th})	$C_{\mathrm{tot,ann}}$ (M£)	$C_{\mathrm{cap,ann}}$ (M£)	$C_{\mathrm{sav,ann}}$ (M£)	t_{PBT} (years)	$\mathcal{E}_{\mathrm{sav,CO_2}}$ (%)
High-spec domestic ASHP systems	3	2.8 (electric heater)	66	4.9	61	-1.1	-	59
Low-spec domestic ASHP systems	3	2.8 (electric heater)	78	7.7	48	-4.7	-	47

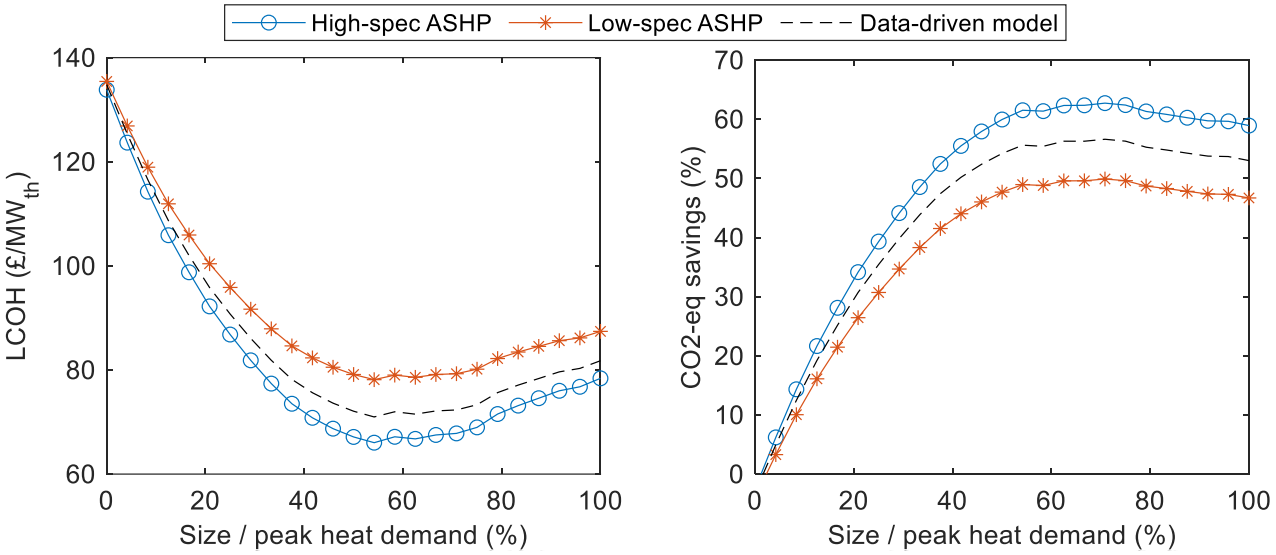


Figure 14. Comparison of two ASHP pathways in terms of: (a) LCOH; and (b) total investment cost, for varying technology size. The latter is normalised to peak heat demand. Results from the data-driven model are included.

The comparison of the economic and environmental performance of the two heat pump designs, shown in Table 5, reveals that, despite a high-spec-ASHP capital cost more than 25% higher than that of the low-spec option, the total annualised energy cost is significantly lower (£4.9M compared to £7.7M). The LCOH is calculated to be 66 £/MWh_{th}, which is lower than that of the low-spec option (78 £/MWh_{th}), but also than the one obtained with the data-driven model (72 £/MWh_{th}), as shown in Fig. 14. The difference between the CO_2-equivalanet savings potential of the high-spec and low-spec options is significant (~12%), showing that the high-spec solution is a worthwhile investment.

3.4. Uncertainty analysis

This section assesses how cost and performance assumptions can affect the total annualised energy cost $C_{\mathrm{tot,ann}}$ and the CO_2-equivalent savings $\mathcal{E}_{\mathrm{sav,CO_2}}$. This is done by conducting an uncertainty propagation analysis as illustrated by Holman [76]. The uncertainty u_{R} of a result R is equal to:

$$u_R{}^2 = \left[\left(\frac{\partial R}{\partial x_1}u_1\right)^2 + \left(\frac{\partial R}{\partial x_2}u_2\right)^2 + \cdots + \left(\frac{\partial R}{\partial x_n}u_n\right)^2\right], \tag{26}$$

where $x_1, x_2 .. x_{\mathrm{n}}$ are the independent variables and $u_1, u_2 .. u_{\mathrm{n}}$ the absolute uncertainties of them.

This analysis focuses only on two main factors: (i) the investment costs; and (ii) the COP of ASHPs. There are three main reasons for the focus on ASHPs: (i) the data-driven ASHP model is associated with the highest uncertainties amongst all data-driven models (Table 1, Section 2.1.1.4); (ii) the analysis in Section 3.2 reveals that ASHPs deliver improved environmental benefits, achieving CO_2-equivalent savings of >55% compared to <6% from gas-fired CHP systems; and (iii) the objective is to demonstrate the significance of reducing uncertainties specifically in technology characteristics. The latter are epistemic in nature and, as such, can be reduced by increasing the level of detail and/or gathering more data [77]. On the other hand, uncertainties associated to future electricity or gas prices are irreducible (categorised as aleatory) and are excluded from this uncertainty analysis.

First, the optimisation problem is solved and associated uncertainty bounds are calculated using a black-box model: a set of simplified assumptions, which do not utilise the models developed in this work and do not capture the effects of size and off-design operation. In this simplified analysis, the inputs and their uncertainty are set to the average and maximum/minimum values that represent ASHP commercial units: (i) the COP is set to 3 ± 1.5; and (ii) the specific cost is set to 500 ± 400 £/kW_{th}. The process is then repeated using the developed data-driven heat pump model and its associated uncertainty bounds (Table 1, Section 2.2.1.4). Lastly, the uncertainty associated with the validated thermodynamic and component-costing heat pump model is used to evaluate the bounds on the results of the high-spec and low-spec heat pump designs discussed in Section 3.4. The results of uncertainty propagation are reported in Table 6.

Table 6. Total annualised energy cost $C_{\mathrm{tot,ann}}$ (M£) and CO_2-equivalent savings $\mathcal{E}_{\mathrm{sav,CO_2}}$ (%) with uncertainty bounds for the domestic ASHP pathway, in the case of: (i) black-box heat pump model (educated guess on cost and performance); (ii) data-driven heat pump model (from collected data); and (iii) the thermodynamic and component-costing heat pump model for a high-spec and low-spec ASHP.

Pathway	$\boldsymbol{C_{\mathrm{tot,ann}}}$ **(M£)**	$\boldsymbol{\mathcal{E}_{\mathrm{sav,CO_2}}}$ **(%)**
Black-box model	5.2 ± 6.9	58 ± 17
Data-driven model	6.1 ± 4.6	55 ± 11
Thermodynamic model (high-spec heat pump)	4.9 ± 1.1	59 ± 3.4
Thermodynamic model (low-spec heat pump)	7.7 ± 1.6	47 ± 4.7

Table 6 demonstrates that, when compared to a black-box model, the heat pump data-driven model can lead to different results with significantly reduced uncertainties. While the uncertainty levels on $C_{\mathrm{tot,ann}}$ and $\mathcal{E}_{\mathrm{sav,CO_2}}$ reduce by about 33% and 35%, respectively, they remain relatively high, which reflects the large range of possible ASHP designs. When the heat pump thermodynamic model is used, however, the range of different designs can be captured, and uncertainties drop significantly (>70% compared to data-driven model), demonstrating the significance of capturing technology characteristics in system modelling efforts.

3.5. Gas versus electricity price

The value of CHP systems and heat pumps in the effort to decarbonise heating greatly depends on the relative price between gas and electricity. In order to examine this, the optimised-sizes obtained for the thermodynamic domestic-size high-spec ASHP model and the data-driven centralised CHP model are used to obtain results for various price scenarios and Fig. 15 reports the total annualised energy cost for different gas and average electricity price scenarios.

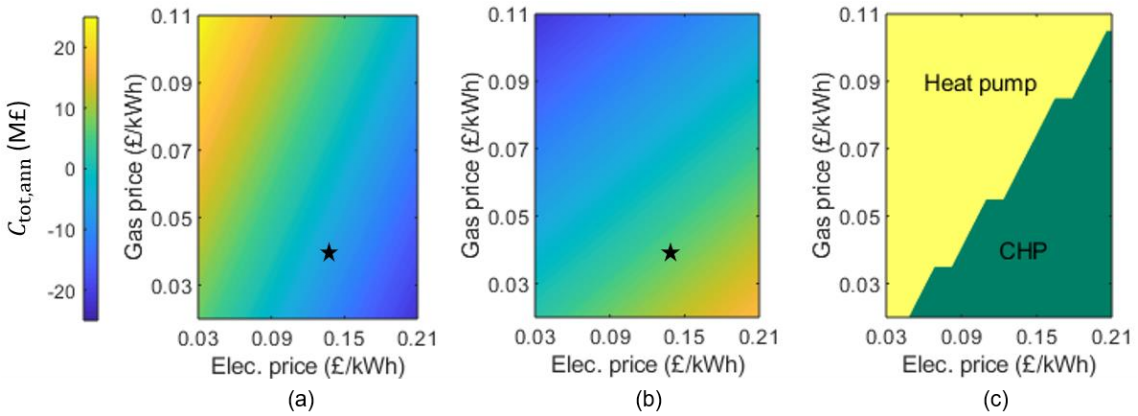


Figure 15. Comparison of economic performance of centralised CHP system versus domestic heat pumps for varying gas and electricity prices: (a) total annualised energy cost $C_{\mathrm{tot,ann}}$ for centralised CHP system; (b) total annualised energy cost $C_{\mathrm{tot,ann}}$ for domestic ASHP; and (c) most cost-effective option for different price ranges. The star represents the current state of prices in the UK (2020).

It appears clearly in Fig. 15 that, when the price of electricity is high compared to that of gas, CHP systems become a worthwhile investment from an economic perspective. On the other hand, heat pumps become competitive when the electricity-to-gas price ratio reduces below about 3. The current energy prices in the UK imply that a CHP system is a more cost-effective option. However, changes in the gas and electricity prices, or relevant energy polices can cause the economic comparison between the two heat generation solutions to change notably. The fact that electrically powered heat pumps can now achieve a much higher degree of decarbonisation than gas-fired CHP systems is of interest and should be considered in developing national energy strategies and policy.

4. Conclusions

Addressing the economic and environmental challenges associated with the provision of low-carbon heat requires models that can examine the trade-offs between different options. In this paper, the variations in the performance and cost of CHP systems and heat pumps with scale (size, rating) and operating conditions are captured with data-driven models based on an extensive analysis of commercially available products on the UK, while a comprehensive thermoeconomic (thermodynamic and costing) model is proposed for the ASHP systems for which the large number of design options results in a large variability (scatter) of available performance and cost data, even at the same scale.

These models are used to compare three main heat-provision pathways: (i) centralised gas-fired CHP system; (ii) middle-scale generation through gas-fired CHP systems or GSHPs for differentiated energy communities; and (iii) distributed micro-CHP units, ASHPs or GSHPs in each household. The Isle of Dogs area in London, UK, is used as a case study for this comparison. The economic and environmental performance of the pathways are evaluated in terms of a set of KPIs. Furthermore, the thermoeconomic ASHP model, which is validated against manufacturer data, allows the comparison of two alternative heat pump designs: a high-cost, high performance one, based on large heat exchangers and working fluid R32; and a low-cost, low-performance one, based on small heat exchangers and working fluid R410a. The novelty of this work lies in the use of the developed technoeconomic models (data-driven, thermodynamic, sizing/costing) to capture realistic technology characteristics (size/scale effects, design characteristics, and off-design operation), therefore providing an informed comparison of possible technology selection and design/sizing options. Furthermore, an uncertainty propagation analysis is conducted to quantify the uncertainty on the results of using the different fidelity approaches.

Results demonstrate that a centralised gas-fired CHP system is the most profitable option in the case of Isle of Dogs, with a LCOH of 31 £/MWh$_{th}$. However, if the carbon footprint factor of grid electricity

continues to increase based on current trends, CHP systems can only provide reduced environmental benefits when compared to boilers (between -1.3% and 5.6%), while domestic ASHPs can reduce carbon emissions by more than 55%. Despite the fact that GSHPs installed at the energy community-level require double the investment cost of domestic ASHPs, they show similar economic performance (LCOH of 74 £/MWh_{th} and 72 £/MWh_{th}, respectively), and higher emission reductions (60%). The use of the thermodynamic heat-pump model allows for an interesting observation; high-specification ASHPs, although more expensive, show higher environmental but also higher economic benefits than lower-specification ASHPs (LCOH of 66 £/MWh_{th} *vs.* 78 £/MWh_{th}, respectively; and CO_2-eq. savings of 59% *vs.* 47%, respectively). An uncertainty propagation analysis demonstrates that a lack of proper accounting of cost and performance variations of heat pumps results in an uncertainty in the total annualised system cost above 100% (5.2 ± 6.9 M£). The utilisation of data-driven models results in a different value and also reduced uncertainty (6.1 ± 4.6 M£), while first-principles models can reduce uncertainties by more than 75%, (4.9 ± 1.1 M£ for the high-spec ASHP case) therefore providing more meaningful results, upon which stakeholders can base their decisions. Lastly, a gas and electricity price sensitivity shows that energy prices play a key role in the comparison of the economic potential of CHP and heat pump systems and the analysis provides evidence to support energy policy.

Acknowledgments

This work was supported by the UK Natural Environment Research Council (NERC) [grant number NE/L002515/1] and the UK Engineering and Physical Sciences Research Council (EPSRC) [grant number EP/R045518/1]. The authors would also like to acknowledge the Science and Solutions for a Changing Planet Doctoral Training Partnership (SSCP DTP). A short version of this paper was presented at the 11th International Conference on Applied Energy (ICAE2019) held on 12-15 August 2019 in Västerås, Sweden. This paper is a substantial extension of the short version of the conference paper. Data supporting this publication can be obtained on request from cep-lab@imperial.ac.uk.

References

[1] Olympios AV, Pantaleo AM, Sapin P, van Dam KH, Markides CN. Centralised vs distributed energy systems options: district heating for the Isle of Dogs in London. In Proc: 11th International Conference on Applied Energy (ICAE 2019), Västerås, Sweden; 2019.
[2] Committee on Climate Change (CCC). Net Zero: The UK's contribution to stopping global warming. 2019.
[3] Fragaki A, Markvart T, Laskos G. All UK electricity supplied by wind and photovoltaics – The 30–30 rule. Energy 2019; 169: 228–37.
[4] Committee on Climate Change (CCC). Next steps for UK heat policy. 2016.
[5] Department of business, energy & industrial strategy. Energy consumption in the UK. 2018.
[6] Hansen K, Breyer C, Lund H. Status and perspectives on 100% renewable energy systems. Energy 2019; 175: 471–80.
[7] Shaik S, Yeboah OA. Does climate influence energy demand? A regional analysis. Appl Energy 2018; 212: 691–703.
[8] Department of Energy & Climate Change (DECC). The future of heating: A strategic framework for low carbon heat in the UK. 2012.
[9] Kannan R. The development and application of a temporal MARKAL energy system model using flexible time slicing. Appl Energy 2011; 88(6): 2261–72.
[10] Kannan R, Strachan N. Modelling the UK residential energy sector under long-term decarbonisation scenarios: comparison between energy systems and sectoral modelling approaches. Appl Energy 2009; 86(4): 416–28.
[11] Strbac G, Pudjianto D, Sansom R, Djapic P, Ameli H, Shah N, Hawkes A. Analysis of alternative UK heat decarbonisation pathways. 2018.
[12] Pfenninger S, Hawkes A, Keirstead J. Energy systems modeling for twenty-first century energy challenges. Renew Sustain Energy Rev 2014; 33: 74–86.

[13] Samsatli S, Samsatli NJ. A multi-objective MILP model for the design and operation of future integrated multi-vector energy networks capturing detailed spatio-temporal dependencies. Appl Energy 2018; 220: 893–920.
[14] Samsatli S,Samsatli NJ. A general spatio-temporal model of energy systems with a detailed account of transport and storage. Comput Chem Eng 2015; 80: 155–76.
[15] Sachs J, Meng Y, Giarola S, Hawkes A. An agent-based model for energy investment decisions in the residential sector. Energy 2019; 172: 752–68.
[16] Heuberger CF, Staffell I, Shah N, Mac Dowell N. A systems approach to quantifying the value of power generation and energy storage technologies in future electricity networks. Comput Chem Eng 2017; 107: 247–56.
[17] Heuberger CF, Rubin ES, Staffell I, Shah N, Mac Dowell N. Power capacity expansion planning considering endogenous technology cost learning. Appl Energy 2017; 204: 831–45.
[18] Markides CN. The role of pumped and waste heat technologies in a high-efficiency sustainable energy future for the UK. Appl Therm Eng 2013; 53: 197–209.
[19] Acha S, Mariaud A, Shah N, Markides CN. Optimal design and operation of distributed low-carbon energy technologies in commercial buildings; Energy 2018; 142: 578–91.
[20] Fischer D, Madani H. On heat pumps in smart grids: A review. Renew Sustain Energy Rev 2017; 70: 342–57.
[21] Chatzopoulou MA, Simpson MC, Sapin P, Markides CN. Off-design optimisation of organic Rankine cycle (ORC) engines with piston expanders for medium-scale combined heat and power applications. Appl Energy 2019; 238: 1211–36.
[22] Department of Energy & Climate Change (DECC). Summary evidence on district heating networks in the UK. 2013.
[23] Hansen CH, Gudmundsson O, Detlefsen N. Cost efficiency of district heating for low energy buildings of the future. Energy 2019; 177: 77–86.
[24] Pirouti M, Bagdanavicius A, Ekanayake J, Wu J, Jenkins N. Energy consumption and economic analysis of a district heating network. Energy 2013; 57: 149–59.
[25] Delangle A, Lambert RSC, Shah N, Acha S, Markides CN. Modelling and optimising the marginal expansion of an existing district heating network. Energy 2017; 140:209–23.
[26] van Der Schoor T, Scholtens B. Power to the people: Local community initiatives and the transition to sustainable energy. Renew Sustain Energy Rev 2015; 43: 666–75.
[27] Mathworks, Optimization toolbox user's guide. 2019.
[28] Department for Communities and Local Government. English housing survey. 2014.
[29] Helen Charlick, Iain Summerfield. Investigation of the interaction between hot water cylinders, buffer tanks and heat pumps. Kiwa Ltd. 2013.
[30] Brooke SB, Matthews D, Willson C. UK literature review for: International Energy Agency (IEA) annex 36 on investigating the effect of quality of installation and maintenance on heat pump performance. 2013.
[31] Ministry of Housing, Communities & Local Government. Land use statistics by ward (generalised land use database), 2018. https://data.london.gov.uk/dataset/land-use-ward.
[32] Dodd N. Community energy: urban planning for a low carbon future. The combined heat and power association (CHPA). 2008.
[33] Simpson MC, Chatzopoulou MA, Oyewunmi OA, Le Brun N, Sapin P, Markides CN.Technoeconomic analysis of internal combustion engine – organic Rankine cycle systems for combined heat and power in energy-intensive buildings. Appl Energy 2019; 113462.
[34] Chatzopoulou MA, Markides CN. Thermodynamic optimisation of a high-electrical efficiency integrated internal combustion engine – organic Rankine cycle combined heat and power system. Appl Energy 2018; 226: 1229–51.
[35] Olympios AV, Le Brun N, Acha S, Lambert RSC, Shah N, Markides CN. Installation of a dynamic controller for the optimal operation of a CHP engine in a supermarket under uncertainty. In Proc: 32nd International Conference on Efficiency, Cost, Optimisation, Simulation and Environmental Impact of Energy Systems (ECOS 2019), Wrocław, Poland; 2019.
[36] Department of Energy & Climate Change (DECC). Heat pumps in district heating. 2016.

[37] Huang MJ, Hewitt NJ. The experimental analysis of the effect of ambient factors on the defrosting of economised vapour injection compressor air source heat pump in marine climates. Int J Refrig 2013; 36(3): 820–27.
[38] Van Kenhove E, De Vlieger P, Laverge J, Janssens A. Towards energy efficient and healthy buildings: trade-off between Legionella pneumophila infection risk and energy efficiency of domestic hot water systems. In 12th REHVA world congress, Aalborg, Denmark; 2016.
[39] Montgomery DC,Runger G. Applied Statistics and Probability for Engineers. John Wiley & Sons. 2010.
[40] Moré JJ. The Levenberg-Marquardt algorithm: Implementation and theory. In Conference on numerical analysis, Dundee, UK; 1977.
[41] Bellos E, Tzivanidis C. Multi-objective optimization of a solar assisted heat pump-driven by hybrid PV. Appl Therm Eng 2019; 149: 528–35.
[42] Olalekan WS, Hakim L. Suitability of difluoromethane refrigerant (R32) as a better alternative refrigerant to puron (R410A) in a refrigeration and air conditioning system. Jour Adv Res Dyn Control Syst 2019; 11(2): 68-74.
[43] Grant, Wave cylinder range: high efficiency direct and indirect hot water storage solutions. 2018. https://www.grantuk.com/media/2971/grant-cylinder-range-brochure-august-2018.pdf
[44] Greater London Authority (GLA). Decentralised energy capacity study - phase 3: Roadmap to deployment. 2011. https://www.london.gov.uk/sites/default/files/gla_migrate_files_destination/de_study_phase3_0_0.pdf.
[45] Parsons Brinckerhoff. Upper Lee Valley network pre-feasibility decentralised energy study. 2011.
[46] Astolfi M. Techno-economic optimization of low temperature CSP systems based on ORC with screw expanders. Energy Procedia 2015; 69: 1100–12.
[47] BITZER Kühlmaschinenbau GmbH. BITZER Software. 2020. https://www.bitzer.de/websoftware.
[48] Freeman J, Hellgardt K, Markides CN. An assessment of solar-powered organic Rankine cycle systems for combined heating and power in UK domestic applications. Appl Energy 2015; 138: 605–20.
[49] Lecompte S, Huisseune H, van den Broek M, De Schampheleire S, De Paepe M. Part load based thermo-economic optimization of the organic Rankine cycle (ORC) applied to a combined heat and power (CHP) system. Appl Energy 2013; 111: 871–81.
[50] Carel. Electronic expansion valves & drivers. 2014. https://www.airefrig.com.au/file/price_guide/2014_mar/333-334,388.pdf.
[51] Department of Energy & Climate Change (DECC). Potential cost reductions for air source heat pumps. 2016.
[52] Jenkins S. Economic indicators: CEPCI, chemical engineering essentials for the CPI professional. 2020. https://www.chemengonline.com/economic-indicators-cepci/.
[53] Mitsubishi Electric. Ecodan monobloc air source heat pumps, 2020. https://library.mitsubishielectric.co.uk/pdf/book/PUHZ-HW50-140VHA2-YHA2#page-1-2.
[54] Panasonic. New Aquarea range 2019 - 2020. 2019. http://www.oceanairuk.com/wp-content/uploads/2019/04/Panasonic_A2W_price_list_2019.pdf.
[55] Park N. Middle super output area population estimates. 2019. https://www.ons.gov.uk/peoplepopulationandcommunity/populationandmigration.
[56] Department of Energy & Climate Change (DECC). Socio-economic data for MLSOA, IGZ and LLSOA electricity and gas estimates, 2013. https://www.gov.uk/government/statistical-data-sets/socio-economic-data-for-mlsoa-igz-and-llsoa-electricity-and-gas-estimates.
[57] Bustos-Turu G, van Dam KH, Acha S, Shah N. Load forecasting of electricity and heat demands in urban areas via agent-based modelling, 2016. http://www.imperial.ac.uk/energy-futures-lab/industry/flexifund/flex-1.
[58] Department of Energy & Climate Change (DECC). Lower and middle super output areas electricity consumption, 2016. https://www.gov.uk/government/statistics/lower-and-middle-super-output-areas-electricity-consumption.
[59] Department of Energy & Climate Change (DECC). Lower and middle super output areas gas consumption, 2016. https://www.gov.uk/government/statistics/lower-and-middle-super-output-areas-gas-consumption.
[60] Hevac. Industrial price list. 2020. http://www.hevac.ie/v4/0940aa0c-5421-4a9b-840d-c9a2ae5d95bb/uploads/commercial_price_list_01_01_2014.pdf.

[61] Cedillos Alvarado D, Acha S, Shah N, Markides CN. A technology selection and operation (TSO) optimisation model for distributed energy systems: Mathematical formulation and case study. Appl Energy 2016; 180: 491–503.
[62] Centrica business solutions. A guide to CHP unit sizing. 2017.
[63] Staffell I, Brett D, Brandon N, Hawkes A. A review of domestic heat pumps. Energy Environ Sci 2012; 5(11): 9291–306.
[64] CIBSE. Heat networks: Code of practice for the UK. 2015.
[65] Crawley Borough Council. District heating network engineering assessment. 2016. http://www.crawley.gov.uk/pub_livx/groups/webcontent/documents/otherdocs/pub285331.pdf
[66] Nord Pool, Historical market data, 2020. https://www.nordpoolgroup.com/historical-market-data/.
[67] Acha S, Bustos-Turu G, Shah N. Modelling real-time pricing of electricity for energy conservation measures in the UK commercial sector. In Proc: IEEE International Energy Conference (ENERGYCON 2016), Leuven, Belgium; 2016.
[68] Department of Business Energy & Industrial Strategy (BEIS). Government greenhouse gas conversion factors for company reporting. 2019.
[69] National Grid. Carbon intensity API. 2019. https://carbonintensity.org.uk/.
[70] Met Office. Historic station data. 2020. https://www.metoffice.gov.uk/research/climate/maps-and-data/historic-station-data.
[71] ICAX. Grid carbon factors. 2020, https://www.icax.co.uk/grid_carbon_factors.html.
[72] You T, Wu W, Shi W, Wang B, Li X. An overview of the problems and solutions of soil thermal imbalance of ground-coupled heat pumps in cold regions. Appl Energy 2016; 177: 515–36.
[73] Yu T, Liu Z, Chu G, Qu Y. Influence of intermittent operation on soil temperature and energy storage duration of ground-source heat pump system for residential building. In Proc: Proceedings of the 8th International Symposium on Heating, Ventilation and Air Conditioning, Shaanxi, China; 2014.
[74] Xi C, Lin L, Hongxing Y. Long term operation of a solar assisted ground coupled heat pump system for space heating and domestic hot water. Energy Build 2011; 43(8):1835–44.
[75] National Fire Protection Association. Standard system for the identification of the hazards of materials for emergency response. 2017.
[76] Holman JP. Experimental methods for engineers. 8th ed. New York: McGraw-Hill Education, 2012.
[77] Moret S, Codina Gironès V, Bierlaire M, Maréchal F. Characterization of input uncertainties in strategic energy planning models. Appl Energy 2017; 202: 597–617.
[78] Unamba CK, Sapin P, Li X, Song J, Wang K, Shu G, Tian H, Markides CN. Operational optimisation of a non-recuperative 1-kWe organic Rankine cycle (ORC) engine prototype. Appl Sci 2019; 9(15): 3024.
[79] Karthik P, Kumaresan V, Velraj R. Experimental and parametric studies of a louvered fin and flat tube compact heat exchanger using computational fluid dynamics. Alexandria Eng J 2015; 54(4): 905–15.
[80] Bogaert R, Böles A. Global performance of a prototype brazed plate heat exchanger in a large Reynolds number range. Exp Heat Transf 1995: 8(4): 293–311.
[81] Chisholm D, Wanniarachchi AS. Layout of plate heat exchangers. In Proc: ASME/JSME Thermal Engineering Joint Conference, Reno, Nevada; 1991.
[82] Thonon B, Bontemps A. Condensation of pure and mixture of hydrocarbons in a compact heat exchanger: Experiments and modelling. Heat Transf Eng 2002; 23(6): 3–17.
[83] Chang YJ, Wang CC. A generalized heat transfer correlation for louver fin geometry. Int J Heat Mass Transf 1997; 40(3): 533–44.
[84] Cooper MG. Heat flow rates in saturated nucleate pool boiling - A wide-ranging examination using reduced properties. Adv Heat Transf 1984; 16: 157–239.
[85] Osborn L. Average annual humidity for the United Kingdom. 2020. https://www.currentresults.com/Weather/United-Kingdom/humidity-annual.php.

Appendix A. Heat exchanger modelling

Comprehensive HEX models are utilised to estimate the cost of different HEX designs and examine the system's behaviour in off-design conditions. Geometrical parameters of brazed-plate and plate-fin HEXs are obtained from experimental tests of Unamba *et al.* [78] and Karthik *et al.* [79]. The HEXs are discretised into a series of equal-temperature (single-phase regions) or equal-enthalpy (two-phase regions) increments. For each increment i, the overall heat transfer coefficient U_i and hence the required HEX area A_i are calculated using Eqs. (A.1) and (A.2):

$$\frac{1}{U_i} = \frac{1}{\alpha_{\mathrm{inner},i}} + \frac{\Delta x}{\lambda} + \frac{1}{\alpha_{\mathrm{outer},i}}, \tag{A.1}$$

$$\dot{Q}_i = U_i \mathrm{A}_i \mathrm{LMTD}_{\,\iota}. \tag{A.2}$$

The heat transfer coefficients for single-phase heat transfer except the air side of the evaporator are calculated using the Nusselt number Nu, which is a function of the Reynolds Re and Prandtl number Pr, as shown in Eq. (A.3). Coefficients *a, b,* and *c* are obtained from Bogaert *et al.* [80] and Chrisholm *et al.* [81]. Eq. (A.3) is also used in the condenser two-phase region with an equivalent Reynolds number as recommended by Thonon [82]. Similarly, the Colborn factor j is used for single-phase heat transfer on the air side (Eq. (A.4)), where coefficients a and b are obtained from Chang *et al.* [83]. For the evaporator two-phase region, Eq. (A.5) is used, where α_{cb} and α_{nb} represent the heat transfer coefficients attributed to convective boiling (calculated using Bogaert and Chisholm correlations) and nucleate boiling (obtained from Cooper's correlation [84]) respectively.

$$Nu = a\, Re^b Pr^c, \tag{A.3}$$

$$j = a\, Re^b, \tag{A.4}$$

$$\alpha = (\alpha_{\mathrm{cb}}^2 + \alpha_{\mathrm{nb}}^2)^{1/2}, \tag{A.5}$$

The validity of assuming dry air in the evaporator can be tested by altering the ASHP design model to investigate how the COP varies with the relative humidity of the inlet air at design conditions (heat source temperature of 7 °C and heat sink temperature of 55 °C). For a 5 kW_{th} ASHP of the Panasonic Aquarea range [54] with a PPTD of 5 K in both the condenser and evaporator, the model predicts that the COP varies from 3.13 for dry air (relative humidity = 0%) up to 3.21 for highly humid air (relative humidity = 92%, which corresponds to the highest value reported for London [85]). This represents a maximum relative variation of 2.5%, which is lower than other reported uncertainty levels in the paper.

Appendix B. Heat pump component costing

Table B1 presents the heat pump component cost correlations employed in this study.

Table B1. Heat pump component costs.

Component	Dependent variable	Cost (£)	Ref.
Compressor	Compressor work input (kW)	$125\ \dot{W}_{\mathrm{in}}^{\ 0.58}$	[48]
Water pump	Electrical power (kW)	$512\ \dot{W}_{\mathrm{pump}}^{\ 0.46}$	[48]
Brazed-plate HEX	Heat exchanger area (m^2)	$337 + 214\ A$	[48]
Plate-fin HEX	Heat exchanger area (m^2)	$270A$	[49]
Air fan	Frontal area (m^2)	$578A$	[49]
Expansion valve	-	320	[50]
Miscellaneous hardware (control, heat meters, *etc.*)	-	20%	[51]
Profit margin	-	20%	[51]
Tax	-	20%	-